



Contents lists available at ScienceDirect

## Spectrochimica Acta Part A: Molecular and Biomolecular Spectroscopy

journal homepage: [www.elsevier.com/locate/saa](http://www.elsevier.com/locate/saa)

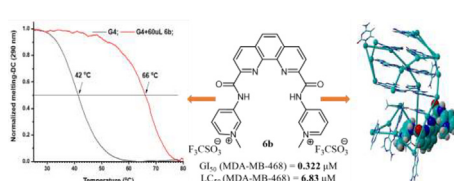
## New 2,9-disubstituted-1,10-phenanthroline derivatives with anticancer activity by selective targeting of telomeric G-quadruplex DNA

Anda-Mihaela Craciun<sup>a,b</sup>, Alexandru Rotaru<sup>b</sup>, Corneliu Cojocaru<sup>b</sup>, Ionel I. Mangalagiu<sup>a</sup>, Ramona Danac<sup>a,\*</sup><sup>a</sup> Chemistry Department, Faculty of Chemistry, "Al. I. Cuza" University of Iasi, 11 Carol I, Iasi 700506, Romania<sup>b</sup> "Petru Poni" Institute of Macromolecular Chemistry, 41A, Grigore Ghica Voda Alley, Iasi 700487, Romania

## HIGHLIGHTS

- New promising anticancer 2,9-disubstituted-1,10-phenanthroline derivatives were developed.
- Compound **5b** displayed GI<sub>50</sub> values < 100 nM against fifteen cancer cell lines.
- Cytotoxic effect was associated with an excellent ability to selectively bind and stabilize G4-DNA.
- CD and molecular docking studies on the interaction of the most active compounds with DNA.

## GRAPHICAL ABSTRACT



## ARTICLE INFO

## Article history:

Received 25 September 2020

Received in revised form 26 November 2020

Accepted 5 December 2020

Available online 14 December 2020

## Keywords:

1,10-Phenanthroline derivatives

Anticancer activity

G-quadruplex ligands

Melting-CD

Heterocycles

Docking

## ABSTRACT

Fifteen new 1,10-phenanthrolines disubstituted at positions 2 and 9 *via* amide bonds with different heterocycles have been designed and synthesized as G-quadruplex DNA stabilizers. Ten compounds were evaluated for the *in vitro* anticancer activity against 60 human tumor cell lines panel, four of them showing a very good inhibitory activity on several cell lines. To assess the ability of the most active compounds to interact with G-quadruplex DNA (G4-DNA), circular dichroism experiments were performed. The potency of the compounds to stabilize the G4-DNA has been shown from the thermal denaturation experiments. The mechanism of compounds binding to DNA and to G4-DNA was theoretically investigated by molecular docking studies.

The experimental results demonstrated excellent capacity of the two compounds bearing two pyridin-3-yl residues (methylated and non-methylated) to act as selective G-quadruplex binders with promising anticancer activity.

© 2020 Elsevier B.V. All rights reserved.

## 1. Introduction

The drug design for anticancer therapy is based on different strategies such as: angiogenesis inhibition, DNA intercalation and groove binding, transcription regulation, enzymes inhibition or microtubules targeting [1]. Among them, one of the most promising strategy that developed rapidly over past years is the intercalation of the G4-DNA that has been recognized in the biologically

functional regions of the human genome such as in the promoter region of some oncogenes that contain G-rich sequences, as well as in the telomers where may have a role in maintaining the chromosome stability [2–5]. Thus, this anticancer approach relies on the formation and stabilization of such G4-DNA structures in the presence of small molecules. In this case, some biological processes as inhibition of telomerase (present in >85% cancer cells of the different lines [6–8]), downregulation the protein expressions or avoiding of the telomere elongation could be affected, thus inducing the cell apoptosis [9–13].

\* Corresponding author.

E-mail address: [rdanac@uaic.ro](mailto:rdanac@uaic.ro) (R. Danac).

The key step for stabilization the telomeric G4-DNA with small molecules, is a good selectivity for human telomeric G4-DNA versus double-stranded DNA (dsDNA) and as well as the necessity to discriminate different G-quadruplexes structures [2].

Recent literature abounds in molecules with a big variety of core structures as acridines, actinomycins, anthracyclines, anthraquinones, quinolones, phenanthridines, phenanthrolines and pyrene, which have been synthesized and proved to have DNA intercalation properties and/or anticancer activity [14–16]. The principal driving forces for intercalation are represented by  $\pi$ - $\pi$  interactions between G-quartets and the aromatic surface of the ligands [17]. Also, the charge-transfer interactions, hydrogen bonding and electrostatic forces play an important role in stabilization of the formed complex [16].

Usually, flat, generally aromatic or heteroaromatic molecules substituted with groups possessing basic functionalities (typically amino groups able to get positively charged at physiological pH) or the presence of the amide NH bond in the molecule which is preferred to form internal H-bonds with nitrogen atoms from heterocycle are promising compounds for G-quadruplex stabilization [2,18].

Several 1,10-phenanthroline derivatives were recently reported as stabilizers of human telomeric G4-DNA, inhibitors of telomerase and showing cytotoxic activity [19–27]. Among them, bisquinolinium derivative Phen-DC<sub>3</sub> (Fig. 1) was the most studied, showing a high selectivity for G-quadruplexes over dsDNAs [19,20].

As a continuation of our work in the field of developing heterocyclic molecules with biological activity [28–31], we present herein, the synthesis of several new small molecules as analogs of Phen-DC<sub>3</sub> (Fig. 1) designed to stabilize G4 structures. The new compounds are derivatives of 1,10-phenanthroline substituted at positions 2 and 9 with different heterocycles connected via amide linkages. Thus, we considered the synthesis of 1,10-phenanthrolines bearing thiazole, pyridine, quinoline or 1,2,3-triazole as substituents at the amidic groups at positions 2 and 9. All these heterocycles were found to be part of molecules showing G4-DNA stabilization properties and/or possessing biological activity [19–22,32–38]. Subsequently, the capacity of the active compounds to interact with dsDNA and G4-DNA was investigated experimentally and by means of theoretical calculations.

## 2. Experimental section

### 2.1. Chemistry

All commercially available reagents and solvents employed were used without further purification. Melting points were recorded on an A. Krüss Optronic Melting Point Meter KSPI and are uncorrected. Proton and carbon nuclear magnetic resonance (<sup>1</sup>H, <sup>13</sup>C) spectra were recorded on a DRX-500 Bruker (500 MHz)

or a Bruker Avance DRX 400 MHz. The following abbreviations were used to designate chemical shift multiplicities: s = singlet, d = doublet, t = triplet, q = quartet, m = multiplet, dd = doublet of doublets, as = apparent singlet. All chemical shifts are quoted on the  $\delta$ -scale in ppm. Coupling constants are given in hertz (Hz). Matrix-assisted laser desorption ionization time of flight (MALDI-TOF) mass spectrometry experiments were carried out on Shimadzu AXIMA Performance operated in high-resolution reflection mode using  $\alpha$ -Cyano-4-hydroxycinnamic acid as matrix. ESI-MS experiments were carried out on Agilent 6520 Accurate-Mass Q-TOF LC/MS. IR spectra were recorded on a FTIR Shimadzu or FTIR Bruker Vertex 70 spectrophotometer. Analyses indicated by the symbols of the elements or functions were within  $\pm 0.4\%$  of the theoretical values. Thin layer chromatography (TLC) was carried out on Merck silica gel 60F<sub>254</sub> plates. Visualization of the plates was achieved using a UV lamp ( $\lambda_{\text{max}} = 254$  or 365 nm). Circular dichroism experiments were recorded by using a Chirascan plus (Applied Photophysics) equipped with a Peltier temperature controller. Spectra were recorded at 25 °C in the wavelength range of 240–340 nm and 240–400 nm.

### 2.2. Procedure for synthesis of compound 2

Neocuproine (14.4 mmol, 1 equiv., 3 g) was dissolved in dioxane (50 mL) and water (2 mL), and the resulting solution was stirred for 20 min. at room temperature. A suspension of selenium dioxide (64.8 mmol, 4.5 equiv., 7.19 g) in a mixture of dioxane (130 mL) and water (5.2 mL) was then added, and the color changed from brown to white. The resulting suspension was refluxed for 24 h, and then the black colored precipitate (selenium metal) was filtered while hot. The resulting solution was cooled and the resulting precipitate was filtered to give the desired compound which was purified by crystallization from acetone.

### 2.3. Procedure for synthesis of compound 3

1,10-Phenanthroline-2,9-dicarbaldehyde **2** (6.3 mmol, 1.5 g) was stirred under reflux for 24 h in 65% HNO<sub>3</sub> (30 mL). The resulting solution was cooled to 0 °C and ice was slowly added to form a yellow precipitate, which was filtered, washed with water and dried. The obtained compound was purified by crystallization from methanol.

### 2.4. Procedure for synthesis of compound 4

To a solution of 1,10-phenanthroline-2,9-dicarboxylic acid **3** (0.373 mmol, 1 equiv., 0.1 g) in anhydrous DCM (10 mL), oxalyl chloride (1.49 mmol, 4 equiv., 0.13 mL) and catalytic anhydrous DMF were added under the inert atmosphere (using N<sub>2</sub>). The solution was refluxed for 24 h. The solvent was removed *in vacuo* to

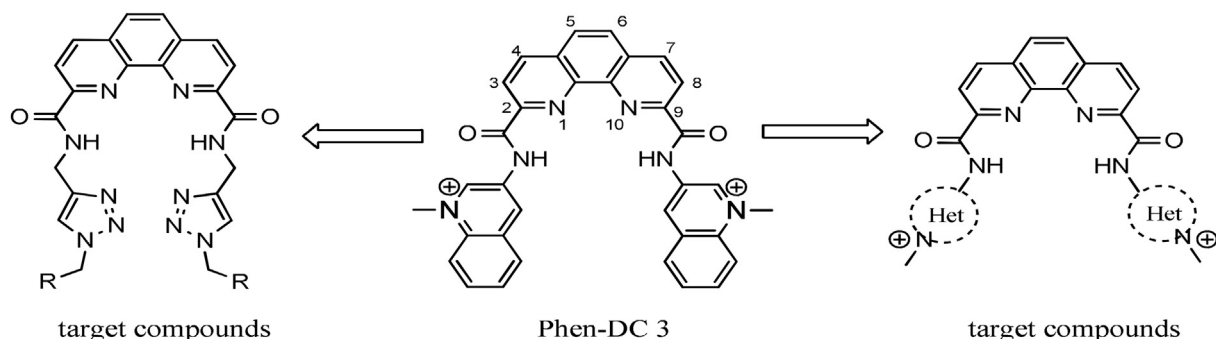


Fig. 1. Structure of Phen-DC<sub>3</sub> and general structures of target compounds.

afford the corresponding 1,10-phenanthroline-2,9-dicarbonyl dichloride which was used immediately in the next step without any purification.

### 2.5. General procedure for the synthesis of compounds **5a-f**

The corresponding amine [propargylamine (0.743 mmol, 2 equiv., 0.05 mL); 2-aminothiazole (0.932 mmol, 2.5 equiv., 0.0932 g); 2-amino-pyridine (0.932 mmol, 2.5 equiv., 0.0876 g); 3-amino-pyridine (0.932 mmol, 2.5 equiv., 0.0876 g); 8-aminoquinoline (0.746 mmol, 2 equiv., 0.107 g); 5-aminoquinoline (0.746 mmol, 2 equiv., 0.107 g)] and triethylamine (TEA) (2.238 mmol, 6 equiv., 0.31 mL) were added to chloroform (5 mL) for synthesis of compounds **5a-c** and **5e** or anhydrous acetonitrile (5 mL) for synthesis of compounds **5d-f**, and the obtained solution was stirred under nitrogen at room temperature for 20 min. 1,10-Phenanthroline-2,9-dicarbonyl dichloride **4** was suspended in 5 mL chloroform (for synthesis of compounds **5a-c** and **5e**) or anhydrous acetonitrile (for synthesis of compounds **5d** and **5f**) and stirred for 15 min., under nitrogen. The solution of the corresponding amine was then added dropwise over the solution of dichloride **4** under nitrogen atmosphere, and the mixture was stirred over night at room temperature. The formed precipitate was collected by filtration and washed with chloroform (for compounds **5a-c** and **5e**) or acetonitrile (compounds **5d-f**). The product was purified by crystallization from dichloromethane/methanol (1:1, v/v).

### 2.6. General procedure for synthesis of compounds **6a-e**

The compound (**5a**, **5b**, **5c** or **5d**) (1 mmol, 1 equiv.) was suspended in chloroform (10 mL) and stirred under reflux (30 min) until the compounds are dissolved. Over the clear solution the trifluoromethanesulfonate agent was added. The optimized conditions involve the next number of equivalents of the methylating agent: for **6a** – 9 equiv., for **6b** and **6e** – 4 equiv. and for **6c** and **6d** – 18 equiv. Immediately after the complete addition of the agent (aprox. 5 min), the precipitate was obtained. This was filtered, washed with chloroform and dried, followed by the structural characterization without any purification.

### 2.7. General procedure for synthesis of compounds **8a-e**

The corresponding 2-bromoacetophenone **7a-e** (1 mmol, 1 equiv.) was dissolved in chloroform (5 mL). Sodium azide (1.1 equiv.), water (2.5 mL) and tetrabutylammonium bromide (0.01 equiv.) were then added. The obtaining reaction mixture was stirred at room temperature for 48 h and then extracted with water (3 x 15 mL), dried on anhydrous Na<sub>2</sub>SO<sub>4</sub> and concentrated in vacuum. The residue was triturated with ethanol and the resulting solid crystallized from ethanol to give the desired compound.

### 2.8. General procedure for synthesis of compounds **9a-e**

N<sup>2</sup>,N<sup>9</sup>-di(prop-2-yn-1-yl)-1,10-phenanthroline-2,9-dicarbonyl dichloride **5f** (0.291 mmol, 1 equiv., 0.1 g), CuSO<sub>4</sub>·5H<sub>2</sub>O (0.146 mmol, 0.5 equiv., 0.04 g) and the corresponding azide **8a-e** were suspended in 20 mL water/*t*-butanol mixture (1/1, v/v) for compounds **9a**, **9b** and **9e** or in 10 mL DMSO/water mixture (4/1, v/v) for compounds **9c** and **9d**. The resulting mixture was stirred for 20 min under nitrogen. Sodium ascorbate (0.087 mmol, 0.3 equiv., 0.017 g) was then added and the obtaining mixture was stirred at 50 °C (for compounds **9a**, **9b** and **9e**) and at 90 °C (for compounds **9c** and **9d**) for 24 h. In case of water/*t*-butanol mixture a precipitate was obtained, while into the DMSO/water mixture, after the reaction time, 10 mL of water was added in order to obtain a precipitate.

The obtained precipitate was filtered and then washed with 10 mL H<sub>2</sub>O/NH<sub>3</sub> (25%) (1/1, v/v) to give the desired compound. The product was purified by crystallization from chloroform/methanol (1:1, v/v).

**1,10-phenanthroline-2,9-dicarbonyl dichloride (2)**. Yellow solid, 85% yield; <sup>1</sup>H NMR (DMSO *d*<sub>6</sub>, 500 MHz): δ = 8.27 (2H, s, H-5), 8.29 (2H, d, *J* = 8.5 Hz, H-3), 8.77 (2H, d, *J* = 8.5 Hz, H-4), 10.34 (2H, s, CHO); <sup>13</sup>C NMR (DMSO *d*<sub>6</sub>, 125 MHz): δ = 120.1 (C-3), 129.2 (C-5), 131.4 (C-6), 138.4 (C-4), 145.3 (C-7), 152.2 (C-2), 193.7 (CHO). Anal. Calcd. for C<sub>14</sub>H<sub>8</sub>N<sub>2</sub>O<sub>2</sub>: C, 71.18; H, 3.41; N, 11.86. Found: C, 71.15; H, 3.38; N, 11.91.

**1,10-phenanthroline-2,9-dicarboxylic acid (3)**. Pale yellow solid, 90% yield; <sup>1</sup>H NMR (DMSO *d*<sub>6</sub>, 500 MHz): δ = 8.1 (2H, s, H-5), 8.42 (2H, d, *J* = 8.5 Hz, H-3), 8.62 (2H, d, *J* = 8.5 Hz, H-4) 9.62 (2H, s, COOH); <sup>13</sup>C NMR (DMSO *d*<sub>6</sub>, 125 MHz): δ = 123.8 (C-3), 128.8 (C-5), 130.5 (C-6), 137.5 (C-4), 142.6 (C-7), 148.3 (C-2), 166.7 (COOH). Anal. Calcd. for C<sub>14</sub>H<sub>8</sub>N<sub>2</sub>O<sub>4</sub>: C, 62.69; H, 3.01; N, 10.44. Found: C, 62.67; H, 3.98; N, 10.41.

**N<sup>2</sup>,N<sup>9</sup>-di(pyridin-2-yl)-1,10-phenanthroline-2,9-dicarboxamide (5a)** [39]. White solid, 45% yield; mp 252–254 °C; IR (KBr), ν<sub>max</sub> 2964, 1687, 1537, 1433 cm<sup>-1</sup>; <sup>1</sup>H NMR (DMSO *d*<sub>6</sub>, 500 MHz): δ = 7.33 (2H, t, *J* = 5.5 Hz, H-13), 8.08 (2H, t, *J* = 8.5 Hz, H-14), 8.23 (2H, s, H-5), 8.44 (2H, d, *J* = 8.5 Hz, H-15), 8.50 (2H, d, *J* = 5.0 Hz, H-12), 8.59 (2H, d, *J* = 8.0 Hz, H-3), 8.81 (2H, d, *J* = 8.0 Hz, H-4), 11.51 (2H, s, NH); <sup>13</sup>C NMR (DMSO *d*<sub>6</sub>, 125 MHz): δ = 114.2 (C-15), 120.2 (C-13), 121.3 (C-3), 128.4 (C-5), 130.9 (C-6), 138.8 (C-4), 140.0 (C-14), 143.4 (C-7), 146.3 (C-12), 148.1 (C-2), 149.9 (C-10), 162.4 (C-8). MALDI-TOF positive mode, *m/z*: 421 [M + H<sup>+</sup>] (100%).

**N<sup>2</sup>,N<sup>9</sup>-di(pyridin-3-yl)-1,10-phenanthroline-2,9-dicarboxamide (5b)**. White solid, 35% yield, mp 294–297 °C; IR (KBr): ν<sub>max</sub> 3238, 3058, 2925, 1675, 1654, 1592, 1541, 1485, 1420, 873, 804, 707 cm<sup>-1</sup>; <sup>1</sup>H NMR (DMSO *d*<sub>6</sub>, 400 MHz): δ = 7.50 (2H, dd, *J* = 8.0; 6.0 Hz, H-14), 8.29 (2H, s, H-5), 8.41 (2H, d, *J* = 4.0 Hz, H-13), 8.52 (2H, d, *J* = 8.4 Hz, H-15), 8.62 (2H, d, *J* = 8.4 Hz, H-3), 8.86 (2H, d, *J* = 8.0 Hz, H-4), 9.28 (2H, bs, H-11), 11.55 (2H, s, NH); <sup>13</sup>C NMR (DMSO *d*<sub>6</sub>, 100 MHz): δ = 121.6 (C-3), 123.6 (C-14), 127.2 (C-15), 128.4 (C-5), 130.7 (C-6), 135.2 (C-10), 138.7 (C-4), 143.6 (C-7), 142.0 (C-11), 144.9 (C-13), 149.3 (C-2), 163.0 (C-8). Anal. Calcd. for C<sub>24</sub>H<sub>16</sub>N<sub>6</sub>O<sub>2</sub>: C, 68.56; H, 3.84; N, 19.99. Found: C, 68.53; H, 3.80; N, 20.05.

**N<sup>2</sup>,N<sup>9</sup>-di(quinolin-5-yl)-1,10-phenanthroline-2,9-dicarboxamide (5c)**. Yellow solid, 15% yield; <sup>1</sup>H NMR (CDCl<sub>3</sub>, 500 MHz): δ = 7.47 (2H, d, *J* = 8.0 Hz, H-13), 7.78 (2H, t, *J* = 8.0 Hz, H-16), 7.93 (2H, d, *J* = 8.0 Hz, H-12), 8.10 (2H, s, H-5), 8.20 (2H, bs, H-17), 8.38 (2H, bs, H-11), 8.60 (2H, bs, H-15), 8.63 (2H, d, *J* = 8.0 Hz, H-3), 8.79 (2H, d, *J* = 8.0 Hz, H-4), 11.29 (2H, s, NH); <sup>13</sup>C NMR (CDCl<sub>3</sub>, 125 MHz): δ = 119.5 (C-11), 120.4 (C-18), 122.0 (C-3), 127.0 (C-12), 127.9 (C-17), 128.3 (C-5), 129.1 (C-13), 129.9 (C-6), 131.5 (C-16), 132.3 (C-10), 138.0 (C-19), 138.6 (C-4), 143.4 (C-7), 149.4 (C-2), 150.0 (C-15), 164.0 (C-8). Anal. Calcd. for C<sub>32</sub>H<sub>20</sub>N<sub>6</sub>O<sub>2</sub>: C, 73.84; H, 3.87; N, 16.14. Found: C, 73.88; H, 3.80; N, 16.20.

**N<sup>2</sup>,N<sup>9</sup>-di(quinolin-8-yl)-1,10-phenanthroline-2,9-dicarboxamide (5d)**. Beige solid, 45% yield; mp 303.9–304.5 °C; IR (KBr) ν<sub>max</sub> 3551, 3477, 3414, 1681, 1638, 1618, 1537, 1486 cm<sup>-1</sup>; <sup>1</sup>H NMR (DMSO *d*<sub>6</sub>, 500 MHz): δ = 6.55 (2H, dd, *J* = 8.5; 4.0 Hz, H-15), 7.57 (2H, d, *J* = 8.0 Hz, H-13), 7.68 (2H, t, *J* = 8.0 Hz, H-12), 7.83 (2H, d, *J* = 3.5 Hz, H-16), 7.85 (2H, d, *J* = 8.0 Hz, H-14), 8.31 (2H, s, H-5), 8.65 (2H, d, *J* = 8.0 Hz, H-3), 8.89 (2H, d, *J* = 7.5 Hz, H-11), 8.90 (2H, d, *J* = 8.0 Hz, H-4), 12.73 (2H, s, NH); <sup>13</sup>C NMR (DMSO *d*<sub>6</sub>, 125 MHz): δ = 116.4 (C-11), 120.6 (C-15), 121.1 (C-3), 122.4 (C-13), 126.6 (C-12), 127.4 (C-19), 128.2 (C-5), 130.6 (C-6), 133.9 (C-10), 135.3 (C-14), 138.3 (C-18), 138.8 (C-4), 143.6 (C-7), 147.5 (C-16), 149.4 (C-2), 162.2 (C-8). MALDI-TOF positive mode, *m/z*: 521 [M + H<sup>+</sup>] (25%); 543 [M + Na<sup>+</sup>] (100%). Anal. Calcd. for

C<sub>32</sub>H<sub>20</sub>N<sub>6</sub>O<sub>2</sub>: C, 73.84; H, 3.87; N, 16.14. Found: C, 73.91; H, 3.82; N, 16.25.

*N*<sup>2</sup>,*N*<sup>9</sup>-di(thiazol-2-yl)-1,10-phenanthroline-2,9-dicarboxamide (**5e**). Yellow solid, 77% yield; mp 348–351 °C; IR (KBr),  $\nu_{\max}$  3365, 3082, 1671, 1562, 1504 cm<sup>-1</sup>; <sup>1</sup>H NMR (DMSO *d*<sub>6</sub>, 500 MHz):  $\delta$  = 7.39 (2H, d, *J* = 3.5 Hz, H-13), 7.65 (2H, d, *J* = 3.5 Hz, H-12), 8.30 (2H, s, H-5), 8.60 (2H, d, *J* = 8.0 Hz, H-3), 8.87 (2H, d, *J* = 8.0 Hz, H-4), 12.87 (2H, s, NH); <sup>13</sup>C NMR (DMSO *d*<sub>6</sub>, 125 MHz):  $\delta$  = 114.6 (C-13), 122.2 (C-3), 128.7 (C-5), 131.0 (C-6), 138.2 (C-12), 138.8 (C-4), 144.1 (C-7), 148.2 (C-2), 157.7 (C-10), 163.1 (C-8). MALDI-TOF positive mode, *m/z*: 433 [M + H<sup>+</sup>] (55%); 455 [M + Na<sup>+</sup>] (100%). Anal. Calcd. for C<sub>20</sub>H<sub>12</sub>N<sub>6</sub>O<sub>2</sub>S<sub>2</sub>: C, 55.55; H, 2.78; N, 19.45. Found: C, 55.58; H, 2.74; N, 19.51.

*N*<sup>2</sup>,*N*<sup>9</sup>-di(prop-2-yn-1-yl)-1,10-phenanthroline-2,9-dicarboxamide (**5f**). Brown solid, 40% yield; mp 250–252 °C; IR (KBr)  $\nu_{\max}$  3405, 3276, 3194, 2925, 1682, 1523, 1492 cm<sup>-1</sup>; <sup>1</sup>H NMR (CDCl<sub>3</sub>, 500 MHz):  $\delta$  = 2.34 (2H, as, H-12), 4.36 (4H, as, H-10), 7.96 (2H, s, H-5), 8.47 (2H, d, *J* = 8.0 Hz, H-4), 8.60 (2H, d, *J* = 8.0 Hz, H-3), 8.82 (2H, s, NH); <sup>13</sup>C NMR (CDCl<sub>3</sub>, 125 MHz):  $\delta$  = 29.6 (C-10), 72.0 (C-12), 79.6 (C-11), 121.8 (C-3), 128.1 (C-5), 130.9 (C-6), 138.1 (C-4), 144.4 (C-7), 149.5 (C-2), 164.1 (C-8). Anal. Calcd. for C<sub>20</sub>H<sub>14</sub>N<sub>4</sub>O<sub>2</sub>: C, 70.17; H, 4.12; N, 16.37. Found: C, 70.19; H, 4.00; N, 16.40.

2,2'-((1,10-phenanthroline-2,9-dicarbonyl)bis(azanediyl))bis(1-methylpyridin-1-ium) trifluoromethanesulfonate (**6a**). White solid, 70% yield, mp 260–264 °C; <sup>1</sup>H NMR (DMSO *d*<sub>6</sub>, 400 MHz):  $\delta$  = 4.38 (6H, s, 2 × CH<sub>3</sub>), 7.99 (2H, t, *J* = 6.4 Hz, H-13), 8.40 (2H, s, H-5), 8.51 (2H, d, *J* = 8.0 Hz, H-15), 8.66–8.70 (4H, overlapped, H-12, H-3), 8.97–8.99 (4H, overlapped, H-14, H-4); <sup>13</sup>C NMR (DMSO *d*<sub>6</sub>, 100 MHz):  $\delta$  = 44.0 (CH<sub>3</sub>), 123.6 (C-15), 123.8 (C-13), 122.4 (C-3), 129.0 (C-5), 131.5 (C-6), 139.4 (C-4), 143.5 (C-7), 145.9 (C-14), 146.8 (C-12), 147.2 (C-10), 147.7 (C-2), 163.7 (C-8). ESI-MS positive mode, *m/z*: 449 [M–H]<sup>+</sup> (100%).

3,3'-((1,10-phenanthroline-2,9-dicarbonyl)bis(azanediyl))bis(1-methylpyridin-1-ium) trifluoromethanesulfonate (**6b**). White solid, 98% yield, mp 302–307 °C; IR (KBr):  $\nu_{\max}$  3266, 3106, 1691, 1599, 1554, 1512, 1460, 1268, 1151, 1030, 638 cm<sup>-1</sup>; <sup>1</sup>H NMR (DMSO *d*<sub>6</sub>, 500 MHz):  $\delta$  = 4.49 (6H, s, 2 × CH<sub>3</sub>), 8.28 (2H, bs, H-14), 8.36 (2H, s, H-5), 8.70 (2H, d, *J* = 7.5 Hz, H-3), 8.87 (2H, bs, H-13), 8.94 (2H, d, *J* = 8.0 Hz, H-4), 9.12 (2H, d, *J* = 8.0 Hz, H-15), 9.80 (2H, s, H-11), 12.05 (2H, s, NH); <sup>13</sup>C NMR (DMSO *d*<sub>6</sub>, 125 MHz):  $\delta$  = 48.7 (CH<sub>3</sub>), 122.2 (C-3), 127.8 (C-14), 129.0 (C-5), 131.4 (C-6), 135.4 (C-15), 137.2 (C-11), 138.4 (C-10), 139.3 (C-4), 140.7 (C-13), 143.8 (C-7), 148.2 (C-2), 163.6 (C-8). ESI-MS positive mode, *m/z*: 435 [M–15]<sup>+</sup> (100%), 449 [M–H]<sup>+</sup> (10%).

5,5'-((1,10-phenanthroline-2,9-dicarbonyl)bis(azanediyl))bis(1-methylquinolin-1-ium) trifluoromethanesulfonate (**6c**). Yellow solid, 95% yield, mp 294–299 °C; IR (KBr):  $\nu_{\max}$  3439, 3286, 3106, 1689, 1523, 1275, 1159, 1030, 795 cm<sup>-1</sup>; <sup>1</sup>H NMR (DMSO *d*<sub>6</sub>, 500 MHz):  $\delta$  = 4.64 (6H, s, 2 × CH<sub>3</sub>), 7.96 (2H, dd, *J* = 8.5; 5.5 Hz, H-16), 8.29–8.32 (4H, m, H-11, H-13), 8.37 (2H, s, H-5), 8.40 (2H, at, *J* = 8.0 Hz, H-12), 8.67 (2H, d, *J* = 8.0 Hz, H-3), 8.94 (2H, d, *J* = 8.0 Hz, H-4), 9.38 (2H, d, *J* = 8.5 Hz, H-17), 9.42 (2H, d, *J* = 5.5 Hz, H-15), 11.96 (2H, s, NH); <sup>13</sup>C NMR (DMSO *d*<sub>6</sub>, 125 MHz):  $\delta$  = 46.0 (CH<sub>3</sub>), 117.1 (C-12), 121.2 (C-16), 122.13 (C-3), 125.4 (C-11), 126.6 (C-18), 128.76 (C-5), 131.1 (C-6), 134.5 (C-10), 135.1 (C-13), 138.9 (C-4), 143.5 (C-7), 143.9 (C-17), 149.0 (C-2), 150.4 (C-15), 154.8 (C-19), 164.1 (C-8). Anal. Calcd. for C<sub>36</sub>H<sub>26</sub>F<sub>6</sub>N<sub>6</sub>O<sub>8</sub>S<sub>2</sub>: C, 50.94; H, 3.09; N, 9.90. Found: C, 50.89; H, 3.04; N, 9.92.

1-methyl-8-(9-(quinolin-8-ylcarbamoyl)-1,10-phenanthroline-2-carboxamido)quinolin-1-ium trifluoromethanesulfonate (**6d**). Yellow solid, 95% yield, mp 273–275 °C; IR (KBr):  $\nu_{\max}$  3508, 3120, 1682, 1539, 1491, 1278, 1261, 1163, 1030 cm<sup>-1</sup>; <sup>1</sup>H NMR (DMSO *d*<sub>6</sub>, 500 MHz):  $\delta$  = 4.86 (3H, s, CH<sub>3</sub>), 6.71 (1H, dd, *J* = 8.0; 4.0 Hz, H-15'), 7.48 (1H, dd, *J* = 8.0; 5.5 Hz, H-15), 7.62 (2H, d, *J* = 8.0 Hz,

H-13'), 7.70 (1H, t, *J* = 8.0 Hz, H-12'), 7.98 (2H, d, *J* = 4.0 Hz, H-16'), 8.04 (1H, d, *J* = 8.0 Hz, H-14'), 8.18 (1H, t, *J* = 8.0 Hz, H-12), 8.28 (1H, d, *J* = 8.0 Hz, H-13), 8.31 (2H, s, H<sub>5</sub>, H-5'), 8.64 (1H, d, *J* = 8.5 Hz, H-3'), 8.67 (1H, d, *J* = 8.0 Hz, H-3), 8.73 (1H, d, *J* = 5.5 Hz, H-14), 8.83 (1H, d, *J* = 7.5 Hz, H-11), 8.87 (1H, d, *J* = 7.5 Hz, H-11'), 8.92 (1H, d, *J* = 8.0 Hz, H-4'), 8.95 (2H, ad, *J* = 8.0 Hz, H-4, H-16), 11.73 (1H, s, H-9), 12.53 (1H, s, H-9'); <sup>13</sup>C NMR (DMSO *d*<sub>6</sub>, 125 MHz):  $\delta$  = 49.9 (CH<sub>3</sub>), 116.7 (C-11'), 121.0 (C-15), 121.2 (C-15'), 121.4 (C-3), (C-3'), 122.6 (C-13'), 127.2 (C-12'), 127.5 (C-19'), 128.1 (C-5), 128.2 (C-5'), 128.6 (C-13), 129.9 (C-12), 130.7 (C-6'), 130.9 (C-6), 131.0 (C-10), 133.2 (C-10'), 133.3 (C-11), 133.6 (C-19), 136.6 (C-14'), 137.8 (C-18'), 139.2 (C-4), 139.3 (C-4'), 143.2 (C-7), 143.3 (C-7'), 147.9 (C-16), 148.2 (C-2), 148.5 (C-16'), 149.6 (C-2'), 151.9 (C-18), (C-14), 161.9 (C-8'), 162.0 (C-8). Anal. Calcd. for C<sub>34</sub>H<sub>23</sub>F<sub>3</sub>N<sub>6</sub>O<sub>5</sub>S: C, 59.65; H, 3.39; N, 12.28. Found: C, 59.61; H, 3.32; N, 12.35.

1-methyl-2-(9-(pyridin-2-ylcarbamoyl)-1,10-phenanthroline-2-carboxamido)pyridin-1-ium trifluoromethanesulfonate (**6e**). White solid, 90% yield, mp 236–242 °C; <sup>1</sup>H NMR (DMSO *d*<sub>6</sub>, 500 MHz):  $\delta$  = 4.79 (3H, s, CH<sub>3</sub>), 7.29 (1H, t, *J* = 6.5 Hz, H-13), 7.89–7.98 (2H, m, overlapped signals, H-13', H-14), 8.17 (2H, s, H-5), 8.26–8.30 (2H, m, H-5', H-15), 8.49 (1H, d, *J* = 8.0 Hz, H-15'), 8.59 (2H, d, *J* = 3.5 Hz, H-12), 8.61–8.66 (3H, m, overlapped signals, H-3, H-3', H-14'), 8.75 (1H, d, *J* = 8.5 Hz, H-4), 8.88 (1H, d, *J* = 8.0 Hz, H-4'), 9.13 (1H, d, *J* = 6.0 Hz, H-12'), 10.89 (1H, s, NH); <sup>13</sup>C NMR (DMSO *d*<sub>6</sub>, 125 MHz):  $\delta$  = 44.3 (Me), 113.3 (C-15), 120.4 (C-13), 122.0 (C-3'), 121.2 (C-15'), 122.2 (C-3), 122.8 (C-13'), 128.4 (C-5), 129.2 (C-5'), 130.8 (C-6'), 131.5 (C-6), 139.2 (C-4), 139.4 (C-4'), 138.8 (C-14), 143.2 (C-7), 143.6 (C-7'), 145.2 (C-12'), 146.2 (C-14), 148.8 (C-12), 147.4 (C-2'), 148.1 (C-2), 148.5 (C-10'), 150.6 (C-10), 162.8 (C-8), 162.8 (C-8'). MALDI-TOF positive mode, *m/z*: 435 [M<sup>+</sup>] (100%).

*N*<sup>2</sup>,*N*<sup>9</sup>-bis((1-(2-(4-bromophenyl)-2-oxoethyl)-1H-1,2,3-triazol-4-yl)methyl)-1,10-phenanthroline-2,9-dicarboxamide (**9a**). Brown powder, 41% yield; mp 181–183 °C; IR (KBr)  $\nu_{\max}$  3550, 3473, 3414, 1658, 1619, 1585, 1540, 1495 cm<sup>-1</sup>; <sup>1</sup>H NMR (DMSO *d*<sub>6</sub>, 500 MHz):  $\delta$  = 4.80 (4H, d, *J* = 5.5 Hz, H-10), 6.11 (4H, s, H-16), 7.56 (4H, d, *J* = 8.5 Hz, H-20), 7.93 (4H, d, *J* = 8.5 Hz, H-19), 8.12 (2H, s, H-12), 8.19 (2H, s, H-5), 8.48 (2H, d, *J* = 8.5 Hz, H-3), 8.75 (2H, d, *J* = 8.0 Hz, H-4), 9.99 (2H, t, *J* = 6.0 Hz, NH); <sup>13</sup>C NMR (DMSO *d*<sub>6</sub>, 125 MHz):  $\delta$  = 34.8 (C-10), 55.8 (C-16), 121.1 (C-3), 125.1 (C-12), 128.0 (C-5), 128.3 (C-21), 130.1 (C-19), 130.3 (C-6), 132.00 (C-20), 133.1 (C-18), 138.3 (C-4), 143.7 (C-7), 144.8 (C-11), 149.4 (C-2), 163.8 (C-8), 191.5 (C-17). MALDI-TOF positive mode, *m/z*: 821/823/825 [M + Na<sup>+</sup>]. Anal. Calcd. for C<sub>36</sub>H<sub>26</sub>Br<sub>2</sub>N<sub>10</sub>O<sub>4</sub>: C, 52.57; H, 3.19; N, 17.03. Found: C, 52.63; H, 3.12; N, 17.20.

*N*<sup>2</sup>,*N*<sup>9</sup>-bis((1-(2-(4-methoxyphenyl)-2-oxoethyl)-1H-1,2,3-triazol-4-yl)methyl)-1,10-phenanthroline-2,9-dicarboxamide (**9b**). Beige solid, 60% yield; mp 240–244 °C; IR (KBr)  $\nu_{\max}$  3327, 3140, 3070, 2930, 1676, 1600, 1239, 1173 cm<sup>-1</sup>; <sup>1</sup>H NMR (CDCl<sub>3</sub>, 500 MHz):  $\delta$  = 3.87 (6H, s, OMe), 4.99 (4H, s, H-10), 5.80 (4H, s, H-16), 6.94 (4H, d, *J* = 8.0 Hz, H-20), 7.80 (2H, s, H-12), 7.92 (6H, m, H-5, H-19), 8.42 (2H, d, *J* = 8.0 Hz, H-4), 8.56 (2H, d, *J* = 8.0 Hz, H-3), 9.45 (2H, s, NH); <sup>13</sup>C NMR (CDCl<sub>3</sub>, 125 MHz):  $\delta$  = 35.6 (C-10), 55.4 (C-16), 55.7 (OMe), 114.4 (C-20), 121.7 (C-3), 124.3 (C-12), 127.1 (C-18), 127.9 (C-5), 130.7 (C-19, C6), 137.8 (C-4), 143.9 (C-11), 144.4 (C-7), 149.9 (C-2), 164.7 (C-21, C = O<sub>amide</sub>), 189.1 (C = O<sub>ketone</sub>). Anal. Calcd. for C<sub>38</sub>H<sub>32</sub>N<sub>10</sub>O<sub>6</sub>: C, 62.98; H, 4.45; N, 19.33. Found: C, 63.00; H, 4.41; N, 19.36.

*N*<sup>2</sup>,*N*<sup>9</sup>-bis((1-(2-(3,4-dimethoxyphenyl)-2-oxoethyl)-1H-1,2,3-triazol-4-yl)methyl)-1,10-phenanthroline-2,9-dicarboxamide (**9c**). White solid, 90% yield, mp 248–250 °C; IR (KBr):  $\nu_{\max}$  3164, 3142, 2936, 1675, 1591, 1518, 1269, 1160, 1019, 871, 629 cm<sup>-1</sup>; <sup>1</sup>H NMR (CDCl<sub>3</sub>, 500 MHz):  $\delta$  = 3.89 (3H, s, OMe), 3.90 (3H, s, OMe), 3.93 (3H, s, OMe), 3.94 (3H, s, OMe), 4.96 (4H, bs, H-10), 5.81 (4H, s, H-16), 6.88 (2H, bs, H-22), 6.46 (2H, bs, H-19), 7.61 (2H, bs,

H-23), 7.83 (2H, s, H-12), 7.91 (2H, s, H-5), 8.42 (2H, d,  $J = 8.0$  Hz, H-4), 8.56 (2H, d,  $J = 8.0$  Hz, H-3), 9.66 (2H, s, NH);  $^{13}\text{C}$  NMR ( $\text{CDCl}_3$ , 125 MHz):  $\delta = 35.7$  (C-10), 55.4 (C-16), 56.2 (OMe), 56.3 (OMe), 110.2 (C-19), 110.4 (C-22), 121.9 (C-3), 123.1 (C-23), 124.5 (C-12), 127.2 (C-18), 127.9 (C-5), 129.5 (C-11), 130.7 (C-6), 137.9 (C-4), 144.4 (C-7), 149.6 (C-2), 150.1 (C-20), 154.6 (C-21), 164.8 (C = O<sub>amide</sub>), 189.3 (C = O<sub>cetone</sub>). Anal. Calcd. for  $\text{C}_{40}\text{H}_{36}\text{N}_{10}\text{O}_8$ : C, 61.22; H, 4.62; N, 17.85. Found: C, 61.33; H, 4.51; N, 17.96.

$N^2,N^9$ -bis((1-(2-oxo-2-(3,4,5-trimethoxyphenyl)ethyl)-1H-1,2,3-triazol-4-yl)methyl)-1,10-phenanthroline-2,9-dicarboxamide (**9d**). White solid, 80% yield, mp 259–260 °C; IR (KBr):  $\nu_{\text{max}}$  3440, 2924, 2853, 1671, 1586, 1542, 1504, 1457, 1415, 1323, 1127, 1001  $\text{cm}^{-1}$ ;  $^1\text{H}$  NMR ( $\text{CDCl}_3$ , 500 MHz):  $\delta = 3.90$  (6H, s,  $2 \times \text{OMe}$ ), 3.92 (3H, s, OMe), 5.01 (4H, bs, H-10), 5.84 (4H, s, H-16), 7.21 (2H, s, H-19, H-23), 7.81 (2H, s, H-12), 7.93 (2H, s, H-5), 8.44 (2H, d,  $J = 8.0$  Hz, H-4), 8.59 (2H, d,  $J = 8.0$  Hz, H-3), 9.46 (2H, s, NH);  $^{13}\text{C}$  NMR ( $\text{CDCl}_3$ , 125 MHz):  $\delta = 35.7$  (C-10), 55.6 (C-16), 56.6 ( $2 \times \text{OMe}$ ), 61.2 (OMe), 105.9 (C-19), (C-23), 121.7 (C-3), 124.3 (C-12), 128.0 (C-5), 129.1 (C-11), 130.8 (C-6), 137.1, (C-18), 137.9 (C-4), 143.9 (C-21), 144.4 (C-7), 149.8 (C-2), 153.5 (C-20), (C-22), 164.7 (C = O<sub>amide</sub>), 189.9 (C = O<sub>cetone</sub>). Anal. Calcd. For  $\text{C}_{42}\text{H}_{40}\text{N}_{10}\text{O}_{10}$ : C, 59.71; H, 4.77; N, 16.58. Found: C, 59.78; H, 4.69; N, 16.66.

$N^2,N^9$ -bis((1-(anthracen-9-ylmethyl)-1H-1,2,3-triazol-4-yl)methyl)-1,10-phenanthroline-2,9-dicarboxamide (**9e**). Yellow solid, 40% yield, mp 202–204 °C; IR (KBr):  $\nu_{\text{max}}$  3368, 3050, 2926, 1665, 1528, 1493, 1170, 1049, 726  $\text{cm}^{-1}$ ;  $^1\text{H}$  NMR (DMSO  $d_6$ , 500 MHz):  $\delta = 4.53$  (4H, d,  $J = 4.5$  Hz, H-10), 6.54 (4H, s, H-16), 7.45–7.53 (8H, m, H-ar), 7.92 (2H, s, H-12), 8.07 (2H, d,  $J = 8.5$  Hz, H-ar), 8.14 (2H, s, H-5), 8.39 (2H, d,  $J = 8.0$  Hz, H-3), 8.52 (2H, d,  $J = 8.5$  Hz, H-ar), 8.63 (2H, s, H-ar), 8.69 (2H, d,  $J = 8.5$  Hz, H-4), 9.67 (2H, t,  $J = 5.5$  Hz, NH);  $^{13}\text{C}$  NMR (DMSO  $d_6$ , 125 MHz):  $\delta = 34.7$  (C-10), 45.4 (C-16), 121.0 (C-3), 122.8 (C-12), 124.0 ( $2 \times \text{CH-ar}$ ), 125.8 (Cq-ar), 125.3 ( $2 \times \text{CH-ar}$ ), 127.0 ( $2 \times \text{CH-ar}$ ), 127.9 (C-5), 128.9 (CH-ar), (Cq-ar), 129.0 ( $2 \times \text{CH-ar}$ ), 130.2 (C-6), 131.0 (Cq-ar), 138.2 (C-4), 143.6 (C-7), 144.5 (C-11), 149.2 (C-2), 163.7 (C-8). Anal. Calcd. for  $\text{C}_{52}\text{H}_{36}\text{N}_{10}\text{O}_4$ : C, 72.21; H, 4.20; N, 16.19. Found: C, 72.28; H, 4.16; N, 16.26.

## 2.9. Cell proliferation assay

The *in vitro* biological tests were performed to the National Cancer Institute (NCI, USA), under the Developmental Therapeutics Program (DTP). The cytotoxicity experiments were performed using a 48 h exposure protocol which consisted of a sulphorhodamine B assay [40].

## 2.10. General protocol for experiments using circular dichroism

The utilised DNA sequences were: G-quadruplex (G<sub>telomer</sub>) – 5'-TTGGGATTGGGATTGGGATTGGGATT- 3' and dsDNA – G<sub>telo</sub> mer + G<sub>telomer</sub> complement (5'-AATCCAATCCAATCCAATCCCAA – 3').

Circular dichroism experiments were recorded by using a Chirascan plus (Applied Photophysics) equipped with a Peltier temperature controller. Spectra were recorded at 25 °C in the wavelength range of 240–340 nm and 240–400 nm.

A scan parameters used were: 1.5 s response time and 0.5 nm bandwidth. The solutions used for the CD experiments: 100  $\mu\text{M}$  G-quadruplex with 2 mM KCl or 100  $\mu\text{M}$  duplex DNA in the TAE solution with pH = 7.4, incubated with 1.5 mM in DMSO of the each ligand. CD melting experiments were performed by using the G4-DNA solutions, in the presence and absence of ligands, using 60  $\mu\text{L}$  of the ligands (1.5 mM in DMSO) at 290 nm in the temperature range between 25 and 80 °C, with an heating rate of 1 °C/min. By using Origin 7.0 software the  $\Delta T_m$  values were

determined ( $\Delta T_m = T_{\text{mwl}} - T_{\text{mG4}}$ , where  $T_{\text{mwl}}$  representing the  $T_m$  value with ligand and  $T_{\text{mG4}}$  representing the  $T_m$  of the G-quadruplex without ligand [41–43]).

## 2.11. Docking study

For molecular docking simulations, the AutoDock VINA method [44] included in the YASARA-Structure program was used [45]. The molecular structure of phenanthroline compounds **5b**, **5d**, **6b**, **6d** and **9e** (ligands) were built and optimized at PM3 semi-empirical level of theory using Hyperchem software [46]. Two receptors were considered in this study, namely, dsDNA oligonucleotide (receptor-1) and a G-quadruplex structure (receptor-2). Details about these receptors are given in the following. First, to simulate DNA oligonucleotide (receptor-1) we considered the Drew-Dickerson dodecamer d(CGCGAATTCGCG) containing 24 nucleotides, which was built and optimized using YASARA tools. Characteristics of Drew-Dickerson dsDNA dodecamer are as follows: (1) molecular weight, 7.43 kDa; (2) radius of gyration, 13.543 Å; (3) molecular surface area, 3551 Å<sup>2</sup> and (4) solvent accessible surface area, 4531 Å<sup>2</sup>.

Second, the configuration of G-quadruplex (receptor-2) was taken from protein data bank site (rcsb.org) by downloading the structure with PDB ID: 2F8U (NMR solution). This structure (PDB ID: 2F8U) is related to G-quadruplex formed in human Bcl-2 promoter (hybrid form) [47]. The second receptor (2F8U) was chosen for this study, because it has similar characteristics with the first receptor (dsDNA). More exactly, characteristics of 2F8U (receptor-2) are as follows: (1) content of 23 nucleotides with the sequence (GGGCGGGGAG-GAATTGGGCGGG); (2) molecular weight, 7.27 kDa; (2) radius of gyration, 10.647 Å; (3) molecular surface area, 3225 Å<sup>2</sup> and (4) solvent accessible surface area, 3876 Å<sup>2</sup>. By comparing values for radii of gyration and molecular surface areas, it can be inferred that the G-quadruplex (2F8U) is a more condensed receptor than the Drew-Dickerson dsDNA dodecamer.

Next, molecular structures of ligands (**5b**, **5d**, **6b**, **6d** and **9e**) and both receptors (dsDNA and 2F8U) were prepared in YASARA environment for molecular docking simulations in implicit water solvent at pH 7.4. Note that, an automatic parameterization procedure (termed "AutoSMILES") for the unknown structures is implemented in the YASARA program. Therefore, this algorithm was employed to generate force field parameters for receptors and the ligands **5b**, **5d**, **6b**, **6d** and **9e**. Simulations were performed using the self-parameterizing knowledge-based YASARA force field [48,49].

During molecular docking simulations, receptors were treated as rigid structures, whereas the ligand was treated as a flexible molecule. The computations (by AutoDock VINA) were done using a number of 100 docking runs followed by the cluster analysis. Generally, docking results are grouped around certain hot spot conformations, and the lowest energy complex in each cluster is saved by the YASARA program. Two complexes belong to different clusters if the ligand RMSD (root-mean-square-deviation) is greater than an imposed minimum value. In this study, we considered the default RMSD limit (for heavy atoms) equal to 5 Å. After clustering all 100 runs, particular complex conformations were found and grouped into 12 clusters and 10 clusters for the systems dsDNA-Ligand and 2F8U-Ligand, respectively. Thus, molecular docking and clustering results suggested multiple hotspots for binding. For each generated complex, the binding energy ( $E_b$ , kcal/mol) as well as dissociation constant ( $K_d$ , nM) was determined.

## 3. Results and discussion

### 3.1. Chemistry

The synthesis of the new derivatives started with the two steps oxidation of neocuproine **1** to 1,10-phenanthroline-2,9-dicar

boxylic acid **3** [50,51]. The key intermediate in the synthesis of the 1,10-phenanthroline derivatives was dicarbonyl dichloride **4** obtained by treating the acid **3** with oxalyl chloride and catalytic dimethylformamide (Scheme 1).

Compounds **5a-f** based on amide bond, have been synthesized in moderate yields (15–77%) by the direct reaction of dichloride **4** with the 2-aminothiazole, 2-aminopyridine, 3-aminopyridine, 5-aminoquinoline, 8-aminoquinoline and propargylamine, respectively (scheme 2).

The attempt to methylate compounds **5a-e** using methyl iodide failed, therefore we used more reactive methyl trifluoromethanesulfonate as methylation reagent (scheme 3). Various molar ratios (from 1:2 to 1:40) of methyl trifluoromethanesulfonate were added to the compounds **5a-e** in chloroform at reflux in order to obtain the corresponding bis-methylated compounds. Regardless of the molar ratio used, in the case of compounds **5b** and **5c**, we obtained only the corresponding *N,N'*-dimethylated compounds **6b** and **6c**, while for the compound **5d**, only the *N*-methylated compound **6d**. In the case of methylation of compound **5a**, we obtained different ratio mixtures of both mono- and dimethylated compounds **6a** and **6e**, depending on the molar ratio of trifluoromethanesulfonate used. The separation of the two compounds proved to be very difficult and only very small quantities of pure compounds could be isolated. Also, in the above conditions, no corresponding methylated compound of **5e** was obtained.

In order to obtain the triazole substituted target compounds (Fig. 1), first the azides **8a-e** were synthesized by substitution of halogenated derivatives **7a-e** by using sodium azide in a biphasic system and tetrabutylammonium bromide (TBAB) as phase transfer catalyst [52] (Scheme 4).

Then, compounds **9a-e** were synthesized via a “click” cycloaddition of azides **8a-e** to the dipropargylated derivative **5f** (Scheme 5). Reactions were carried out using classical conditions (copper (II) sulphate and sodium ascorbate) in a *tert*-butanol/water at 50 °C for the compounds **9a**, **9b**, **9f** and **9e**, while for the compounds **9c** and **9d** we used DMSO/water as solvent at 90 °C and 1,10-phenanthroline as copper ligand.

All synthesized compounds were fully characterized, including the already reported compound **5a** [39]. The shifting of the amide proton over a moderately wide range in NMR spectra of compounds **5** (8.82 – 12.87 ppm) suggests their involvement in H-bonding with the adjacent nitrogen atom of 1,10-phenanthroline or other atoms.

For the *N*-methylated compounds **6a-e**, the most relevant signals observed in NMR spectra to confirm the methylation, were the ones furnished by the protons and carbon of methyl group (the signal of methyl protons appear at 4.38–4.86 ppm, while the signal of carbon at 44–50 ppm).

### 3.2. Biological assay

Twelve of the new compounds (**5a-c**, **5e**, **5f**, **6a**, **6b**, **6d**, **6e**, **9a**, **9c** and **9d**) were selected by National Cancer Institute (NCI) for screening against 60 human tumor cell lines panel at a single dose of 10 μM [40], but unfortunately, due to the difficulties we faced during separation of compounds **6a** and **6e** from the reaction mix-

ture, we were not able to send these two compounds for testing, therefore only ten compounds have been tested. The representative results are summarized in Table 1.

Interestingly, only four compounds, **5b**, **5d**, **6b** and **6d** exhibited a promising growth inhibitory activity against cancer cells. The best growth inhibitory activity was shown by compounds **5b** and **6b**, both of them containing two pyridin-3-yl rings as substituents at the amide groups from positions 2 and 9 of 1,10-phenanthroline. Both compounds showed also cytotoxic activity against several cancer cells, the most important being shown against UACC-62 melanoma cells for compound **6b** and against RXF 393 and A498 renal cancer cells for compound **5b**. We observed that double methylation of **5b** changed the profile of the anticancer activity on the entire panel of cancer cells, being difficult to draw conclusions. It worths also to note, that in Phen-DC<sub>3</sub> (Fig. 1), the position of amino group is also *meta* relative to the heterocyclic nitrogen atom.

Compound **5d** bearing two quinolin-8-yl rests at the two *N*-amide groups showed also a good inhibition effect especially on leukemia and lung cancer cells. Compound **6d** obtained by mono-*N*-methylation of compound **5d** showed also a different profile regarding the inhibitory activity of the cancer cells, but overall, the potency appear to be diminished by comparison with **5d**.

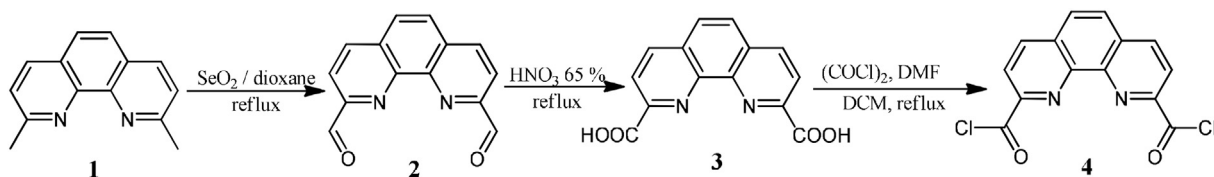
Interestingly, the substitution of *N*-amide with more flexible substituents containing 1,2,3-triazoles in compounds **9** resulted in the loss of the activity, compounds **9a** and **9d** presenting almost no inhibition effect on the tested cell lines. As an exception, compound **9c** showed a very selective moderate activity only against HCT-116 colon cancer cells, M14 melanoma cells and 786-0 renal cancer cells.

Due to the promising shown growth inhibition results, compounds **5b** and **6b** were selected for evaluation against 60 cell lines at five different concentrations. Selected results from the NCI-60 5-dose screen are shown in Table 2.

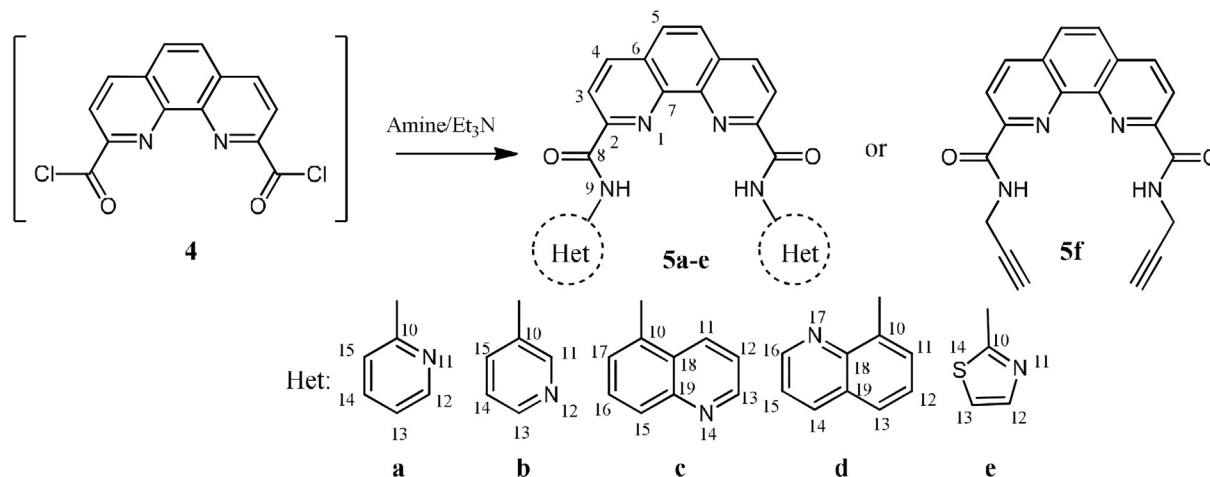
The results presented in Table 2 confirmed the excellent antiproliferative capacity of the compound **5b** that showed GI<sub>50</sub> values much lower than the corresponding dimethylated compound **6b**. Thus, compound **5b** displayed GI<sub>50</sub> values < 100 nM against fifteen cell lines, the best being registered against colon cancer HCC-2998, HCT-116, HCT-15, HT29, KM12 and SW-620 cell lines, lung cancer HOP-62 and NCI-H460 cell lines and leukemia K-562 and HL-60(TB) cell lines.

The best GI<sub>50</sub> values for compound **6b** were obtained against lung cancer NCI-H226 (0.121 μM) and A549/ATCC (0.169 μM) cell lines and renal cancer SN12C (0.126 μM), respectively. Compound **6b** also displayed selective cytotoxic activity on MDA-MB-468 breast cancer cells (LC<sub>50</sub> = 6.83 μM), RXF 393 renal cancer cells (LC<sub>50</sub> = 16.9 μM) and SNB-75 CNS cancer cells (LC<sub>50</sub> = 17.7 μM).

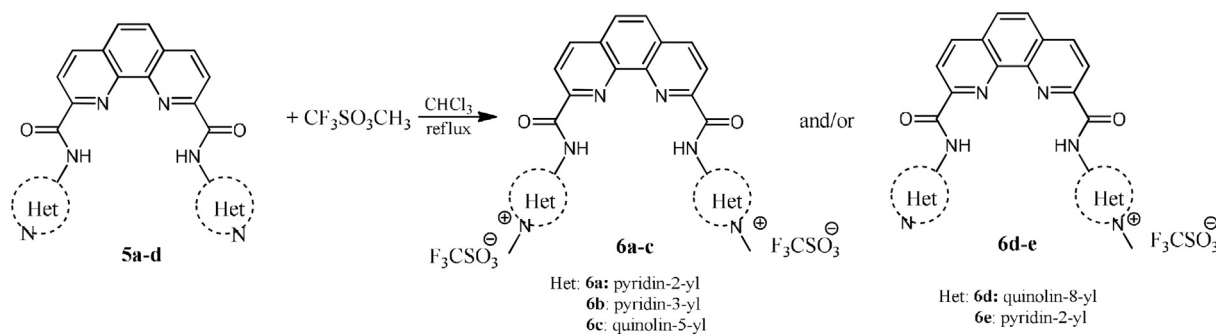
The lethal action shown by compound **6b** on several cancer cells might be explained by its structural particularities leading to possible specific interactions and stabilization of G4-DNA structure. In order to confirm this supposition, circular dichroism experiments were used and the results discussed further. These interactions may induce the inhibition mechanism of telomerase which is up regulated in most cancer subtypes.



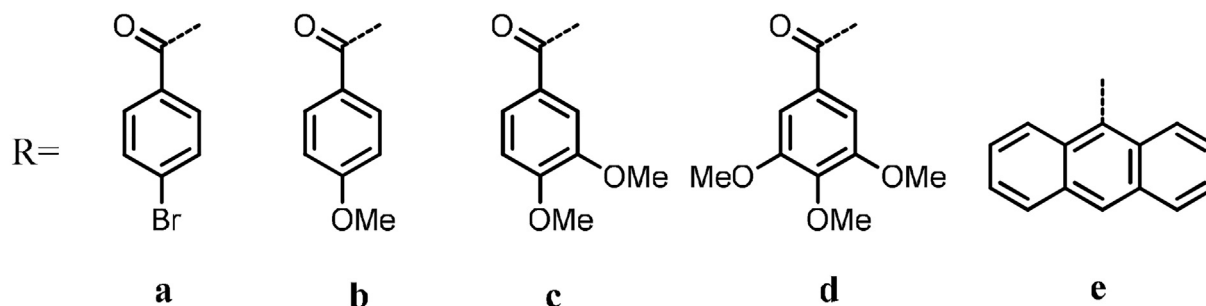
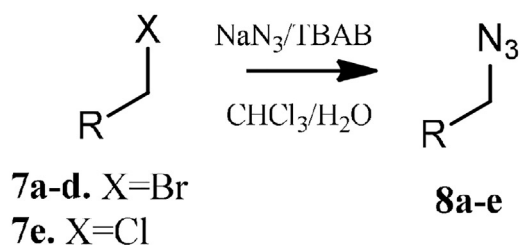
Scheme 1. Oxidation of neocuproine to 1,10-phenanthroline-2,9-dicarboxylic acid **3**.



**Scheme 2.** Synthetic pathway for the 2,9-disubstituted 1,10-phenanthrolines **5a-f**.



**Scheme 3.** Synthetic pathway for the methylated heterocyclic compounds **6a-e**.



**Scheme 4.** Synthetic pathway for azides **8a-e**.

### 3.3. Circular dichroism experiments

In order to evaluate the ability of **5b**, **5d**, **6b**, **6d** and **9e** ligands to interact with DNA (telomeric or duplex), circular dichroism (CD) experiments were used. G-quadruplex structure

was formed from human telomere sequence in the presence of  $K^+$ , when the topology adopted furnished a major positive band at 240 nm and two minor negative bands around 290 nm and 270 nm, this being known as the hybrid [3 + 1] structure of G4-DNA [53].

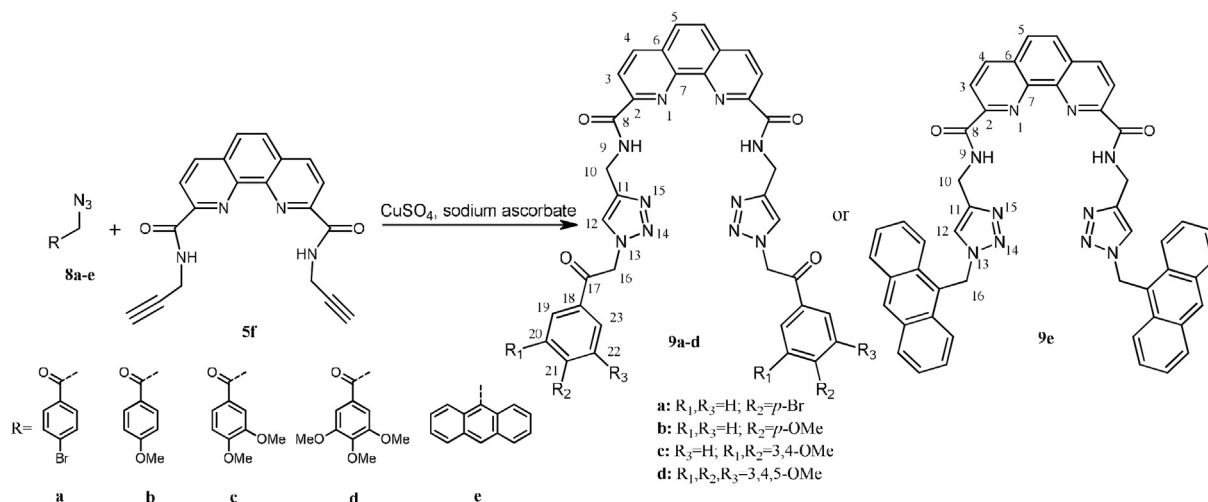


Fig. 2 presents the profiles of the G4–ligand complexes while titrated with solutions of the investigated compounds. Modifying the concentration in case of ligands **5d** and **9e**, respectively, appears to not produce substantial modification of G-quadruplex structures (Fig. 2b,e). Titration with solutions of ligands **6b** and **6d**, respectively, led to significant modification of the starting signal for the G-quadruplex structure (Fig. 2c,d). Thus, for both compounds, a tendency towards an antiparallel conformational structure of G4 could be observed. The antiparallel G4 structure formed for compound **6d** is proved by the 270 nm band that became negative and the 240 nm band that increased to positive values. Also, even if the same structural characteristic aspects could be observed for the compound **6b**, the structure in this case does not fit to a complete antiparallel profile.

However, a different profile of the G-quadruplex structure during the increasing concentration of the ligand **5b** can be observed in Fig. 2a: (i) a slow increasing of the 290 nm and 245 nm bands; (ii) a slow decreasing of the 270 nm band; (iii) the appearance of a new band at 330 nm. This continuous modification of the profile suggests the fact that ligand **5b** did not lead to a stabilization of the G4-DNA structure [19,54].

Slight modifications of the intensities observed in case of all tested compounds can be the result of physical interactions (electrostatic or intermolecular H-bonding) between G4-DNA and ligands.

Next, the ability of the same set of compounds to interact with dsDNA was investigated. dsDNA was prepared by thermal annealing of the single-stranded G-telomer-complement sequence with the G-telomer sequence. The dsDNA formation was proved by CD profile by the presence of characteristic positive band around 270 nm and a negative one around 245 nm. The experimental results with compounds **5b**, **5d**, **6b**, **6d** and **9e** did not show any changes neither in the shape nor the intensity of the original dsDNA signal. This suggests that the interactions are much lower than in the case of the corresponding G4-ligand complex (see Fig. 1S in the supplementary material), thus conferring a great selectivity of investigated **5b**, **6b** and **6d** compounds toward human telomeric G-quadruplex DNA versus duplex DNA.

### 3.4. CD melting experiments

The ability of the studied compounds to stabilize telomeric G4-DNA was further confirmed by using a CD melting assay. In this study, by increasing the temperature (1 °C/min) of the components

solution, the capacity to unfold the DNA-complex structure was registered. Thereby, the melting points between 25 and 80 °C, using an excess (0.45 mM) of compounds solutions, were evaluated and the results are shown in Fig. 3.

By comparing the  $\Delta T_m$  values obtained for the non-methylated derivatives with the methylated ones (Table 3), higher values were obtained in the last cases, indicating a higher ability of **6b** and **6d** to stabilize the G4 structures, data being in agreement to other similar reported results [55,56].

The most promising result, according to the CD melting experiments, was obtained for **6b**, for which the presence of two methyl residues on pyridin-3-yl induced an even higher stabilizing effect, the  $\Delta T_m$  value reaching 24 °C. Typically,  $\Delta T_m$  values higher than 15 °C are required for promising G4 intercalators using different G4 DNA sequences [13,22,56–58].

### 3.5. Docking experiment

To understand the structural basis of the investigated compounds to interact with G-quadruplexes or dsDNA, we performed a series of molecular docking (MD) studies. The AutoDock Vina method implemented in the YASARA Structure software packages [43] was employed for the current MD simulations. Structures of **5b**, **5d**, **6b**, **6d** and **9e** were first drawn and optimized at PM3 level of theory using Hyperchem software [44], and subsequently exported to YASARA program. The structures of G-quadruplex (pdb ID: 2F8U) and dsDNA (pdb ID: 4C64) were used as receptors, dsDNA representing the Drew Deckerson dodecamer [59,60] (assembled in YASARA program). The comparative results of MD simulations indicated the interaction of compounds **5b**, **5d**, **6b**, **6d** and **9e** with both the dsDNA (receptor-1) and G-quadruplex (receptor-2), the selected and optimized molecular docking models being reported in Figures 4, S2-S7 and Table 4.

In both cases, complexes are stabilized mainly by hydrophobic interactions and one hydrogen bond between oxygen atom (from ligand, C = O group) and hydrogen atom (from the receptor, –NH<sub>2</sub> group / A, G residuals) (for details, see ESI). According to these results, the reported compounds interact with receptor-1 by binding predominantly to the minor groove of the dsDNA (Fig. 4) with the theoretically calculated binding energy ( $E_b$ ) for the optimized interactions ranging from –8.24 kcal/mol to –10.57 kcal/mol. The values of theoretically calculated dissociation constant ( $K_d$ ) for the same interactions vary in a larger span, between

**Table 1**  
Percentage growth inhibition (PGI)<sup>a</sup> data of compounds **5a-c**, **5e-f**, **6b**, **6d**, **9a** and **9c-d** at a single concentration (10<sup>-5</sup> M) against an NCI 60 human tumor cell lines (selection).<sup>b</sup>

Panel/Cell line ↓	Compound/Percent growth inhibition (PGI, %)									
	5a	5b	5d	5e	5f	6b	6d	9a	9c	9d
<b>Leukemia</b>										
CCRF-CEM	0	<b>72</b>	<b>62</b>	11	12	29	<b>55</b>	0	0	2
K-562	0	<b>83</b>	44	13	6	<b>65</b>	31	0	0	0
MOLT-4	0	<b>68</b>	<b>60</b>	0	11	28	45	8	0	0
RPMI-8226	0	<b>81</b>	<b>90</b>	12	6	38	<b>56</b>	0	3	3
SR	8	57	<b>61</b>	23	14	25	32	4	0	0
<b>Non-Small Cell Lung Cancer</b>										
A549/ATCC	3	<b>78</b>	58	18	13	<b>100<sup>b</sup> (3)</b>	15	7	0	0
HOP-62	8	<b>91</b>	<b>68</b>	17	11	<b>78</b>	17	0	3	10
HOP-92	0	<b>76</b>	21	0	0	43	1	0	0	0
NCI-H226	4	<b>95</b>	<b>72</b>	19	11	<b>95</b>	12	0	13	0
NCI-H23	0	<b>77</b>	39	11	2	<b>67</b>	13	0	0	1
NCI-H322M	6	<b>89</b>	14	4	9	<b>63</b>	0	10	3	0
NCI-H460	0	<b>98</b>	<b>63</b>	23	0	<b>100<sup>b</sup> (7)</b>	19	0	0	0
NCI-H522	0	<b>70</b>	51	7	17	<b>100<sup>b</sup> (19)</b>	35	16	9	5
<b>Colon Cancer</b>										
COLO 205	0	<b>87</b>	43	7	2	25	18	0	0	0
HCC-2998	0	<b>97</b>	15	20	0	58	15	0	3	4
HCT-116	9	<b>95</b>	<b>62</b>	7	7	57	13	1	<b>78</b>	8
HCT-15	0	<b>80</b>	50	37	1	39	0	0	0	0
HT29	0	<b>93</b>	48	22	8	<b>66</b>	12	3	3	0
KM12	2	<b>94</b>	45	20	2	58	0	0	0	0
SW-620	6	<b>89</b>	28	27	2	44	3	0	0	0
<b>CNS cancer</b>										
SF-268	0	<b>84</b>	39	0	1	47	6	0	0	0
SF-295	1	<b>95</b>	35	9	10	<b>94</b>	4	0	0	0
SF-539	5	<b>100<sup>b</sup> (7)</b>	5	8	6	<b>62</b>	8	0	6	1
SNB-19	0	<b>87</b>	51	8	0	<b>86</b>	30	0	3	8
SNB-75	7	59	0	20	10	<b>87</b>	26	0	8	10
U251	4	<b>88</b>	<b>70</b>	5	6	<b>87</b>	<b>52</b>	2	0	0
<b>Melanoma</b>										
LOX IMVI	0	<b>86</b>	<b>60</b>	23	13	35	31	0	0	0
M14	7	<b>85</b>	42	16	1	46	4	0	<b>63</b>	0
MDA-MB-435	0	<b>75</b>	19	6	0	32	2	0	5	0
SK-MEL-2	0	<b>74</b>	24	12	3	43	16	11	0	1
SK-MEL-28	0	<b>82</b>	10	0	0	<b>68</b>	15	0	0	0
SK-MEL-5	4	<b>74</b>	<b>66</b>	19	13	<b>98</b>	33	0	4	2
UACC-257	1	<b>70</b>	15	3	2	6	1	5	0	0
UACC-62	2	<b>71</b>	47	12	1	<b>100<sup>b</sup> (54)</b>	25	0	9	0
<b>Ovarian cancer</b>										
IGROV1	7	<b>85</b>	28	16	12	<b>67</b>	<b>53</b>	6	0	4
OVCAR-3	0	<b>77</b>	<b>65</b>	0	0	37	8	0	0	0
OVCAR-5	8	<b>63</b>	0	7	3	21	0	3	3	0
OVCAR-8	0	<b>77</b>	50	2	7	38	45	2	0	0
SK-OV-3	0	52	34	1	6	<b>92</b>	12	25	16	5
<b>Renal cancer</b>										
786-0	3	<b>80</b>	40	0	6	23	0	2	<b>57</b>	0
A498	0	<b>100<sup>b</sup> (39)</b>	27	0	0	5	15	0	0	0
ACHN	10	<b>77</b>	44	17	2	58	8	0	0	4
CAKI-1	7	<b>89</b>	46	39	4	47	14	4	13	10
RXF 393	0	<b>100<sup>b</sup> (50)</b>	0	0	0	<b>67</b>	5	0	1	0
SN12C	0	68	30	1	0	<b>100<sup>b</sup> (15)</b>	<b>52</b>	0	2	4
<b>Prostate cancer</b>										
PC-3	0	67	<b>63</b>	19	1	45	23	6	7	0
DU-145	0	<b>85</b>	39	0	0	<b>90</b>	5	0	0	0
<b>Breast cancer</b>										
MDA-MB-231/ATCC	0	<b>75</b>	34	0	0	<b>67</b>	8	2	0	17
HS 578 T	0	54	<b>62</b>	4	0	25	17	0	8	0
MCF7	29	<b>71</b>	26	32	14	54	39	15	3	2
T-47D	20	63	44	23	10	<b>88</b>	48	0	16	11
MDA-MB-468	0	<b>100<sup>b</sup> (2)</b>	23	0	11	<b>100<sup>b</sup> (16)</b>	35	0	4	0

The best values in terms of growth inhibition are highlighted in bold and red.

<sup>a</sup> The number reported for the one-dose assay, percent growth inhibition (PGI) is growth inhibition relative to the no-drug control, and relative to the time zero number of cells.

<sup>b</sup> Cytotoxic effect; Lethality percent is reported in brackets.

17.89 nM and 904.35 nM, revealing a stronger binding of **5d** and **6d** to receptor-1 when compared to **5b**, **6b** and **9e**.

In case of interaction of the ligands **5b**, **5d**, **6b**, **6d** and **9e**, with the receptor-2, the E<sub>b</sub> values were comparable to the ones obtained

for receptor-1, while K<sub>d</sub> values were dramatically different in case of ligand **6b**. A strong decrease in K<sub>d</sub> value from 609.27 nM (receptor-1) to 405.65 nM (receptor-2) shows stronger affinity of ligand **6b** to G-quadruplex, whereas for other ligands, the K<sub>d</sub> values

**Table 2**  
Results of the 5-dose *in vitro* human cancer cell growth inhibition for compounds **11a**, **15a** and **15j** (selection).<sup>a</sup>

Panel/Cell line ↓	Compound/Percent growth inhibition (GI <sub>50</sub> , μM)			
	<b>5b</b>		<b>6b</b>	
	GI <sub>50</sub> (μM)	LC <sub>50</sub> (μM)	GI <sub>50</sub> (μM)	LC <sub>50</sub> (μM)
<b>Leukemia</b>				
CCRF-CEM	0.364	>100	6.860	>100
K-562	<b>0.051</b>	>100	2.100	>100
HL-60(TB)	<b>0.074</b>	>100	2.160	>100
RPMI-8226	0.162	>100	4.040	>100
SR	0.180	>100	4.380	>100
<b>Non-Small Cell Lung Cancer</b>				
A549/ATCC	0.134	>100	<b>0.169</b>	>100
HOP-62	<b>0.083</b>	>100	1.210	>100
NCI-H226	0.128	>100	<b>0.121</b>	>100
NCI-H23	0.219	>100	1.560	>100
NCI-H322M	<b>0.099</b>	>100	2.260	>100
NCI-H460	<b>0.062</b>	>100	<b>0.319</b>	>100
NCI-H522	n.d.	n.d.	0.599	>100
<b>Colon Cancer</b>				
COLO 205	0.135	>100	4.350	>100
HCC-2998	<b>0.065</b>	>100	3.200	>100
HCT-116	<b>0.043</b>	>100	3.070	>100
HCT-15	<b>0.053</b>	>100	4.090	>100
HT29	<b>0.044</b>	>100	2.160	>100
KM12	<b>0.049</b>	>100	3.200	>100
SW-620	<b>0.070</b>	>100	3.280	>100
<b>CNS cancer</b>				
SF-268	0.202	>100	4.290	>100
SF-295	0.237	>100	3.000	>100
SF-539	0.187	>100	3.300	>100
SNB-19	0.106	>100	1.850	>100
SNB-75	0.273	>100	0.521	<b>17.7</b>
U251	<b>0.066</b>	>100	2.440	>100
<b>Melanoma</b>				
LOX IMVI	0.203	>100	6.980	>100
M14	<b>0.080</b>	>100	4.640	>100
MDA-MB-435	0.259	>100	8.690	>100
SK-MEL-28	0.333	>100	1.860	>100
SK-MEL-5	0.229	>100	0.697	>100
UACC-62	0.267	>100	1.450	>100
<b>Ovarian cancer</b>				
IGROV1	0.850	>100	1.360	>100
OVCAR-3	0.243	>100	4.690	>100
OVCAR-8	0.147	>100	5.610	>100
<b>Renal cancer</b>				
786-0	0.337	>100	14.00	>100
A498	0.214	>100	20.30	>100
ACHN	0.155	>100	4.510	>100
CAKI-1	0.141	>100	4.260	>100
RXF 393	0.110	>100	1.980	<b>16.9</b>
SN12C	0.300	>100	<b>0.126</b>	>100
<b>Prostate cancer</b>				
PC-3	<b>0.087</b>	>100	3.620	>100
DU-145	0.177	>100	<b>0.486</b>	>100
<b>Breast cancer</b>				
MDA-MB-231/ATCC	0.511	>100	5.180	>100
MCF7	0.138	>100	2.890	>100
T-47D	0.243	>100	<b>0.395</b>	>100
MDA-MB-468	<b>0.093</b>	>100	<b>0.322</b>	<b>6.83</b>

GI<sub>50</sub> – the molar concentration of tested compound causing 50% growth inhibition of tumor cells.

LC<sub>50</sub> – the molar concentration of tested compound causing 50% death of tumor cells.

n.d. – Not determined.

The best values in terms of GI<sub>50</sub> and LC<sub>50</sub> are highlighted in bold and red.

<sup>a</sup> *In vitro* 60 cell 5-dose screening (from NCI's) [40].

are either comparable for both ligands (**5b**) or higher for G-quadruplex DNA (**5d**, **6d** and **9e**). These data suggest the similar affinity of **5b** to receptor-1 and receptor-2, and stronger affinity of **5d**, **6d** and **9e** to receptor-1 than to receptor-2. Interestingly, the theoretical data obtained for ligand **6b** are supported by the melting point experimental data where **6b** have shown the highest value of  $\Delta T_m$ .

#### 4. Conclusions

A new series of fifteen 1,10-phenanthroline based derivatives designed as analogues of G-quadruplex stabilizer Phen-DC<sub>3</sub> have been synthesized and tested for the anticancer properties and their capacity to selectively stabilizing the G4-DNA structures. Compound **5b** containing two pyridin-3-yl rests as substituents for

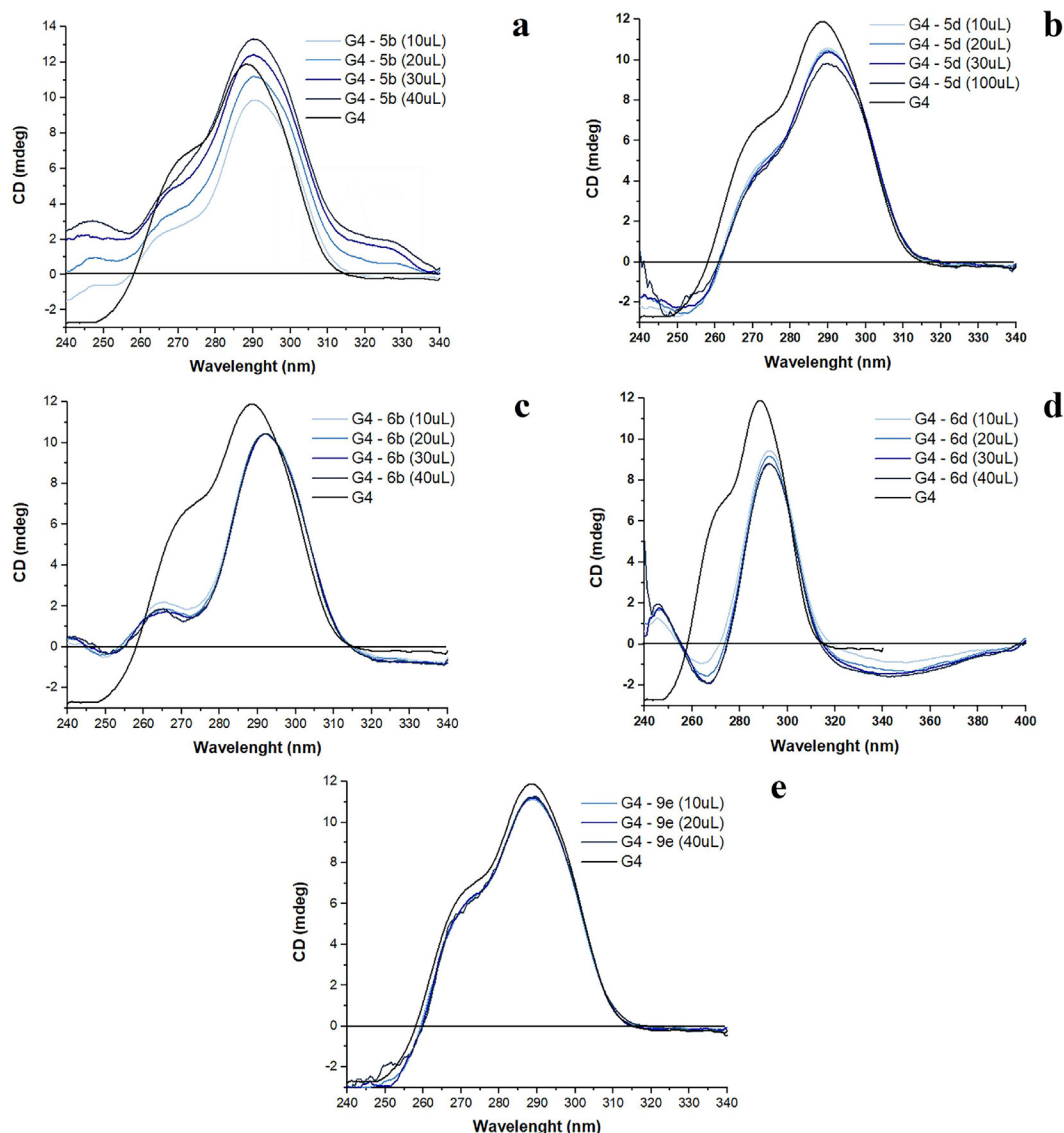


Fig. 2. CD spectra of the G4-DNA in the absence (black line) and in presence of compounds: (a) **5b**; (b) **5d**; (c) **6b**; (d) **6d**; (e) **9e**.

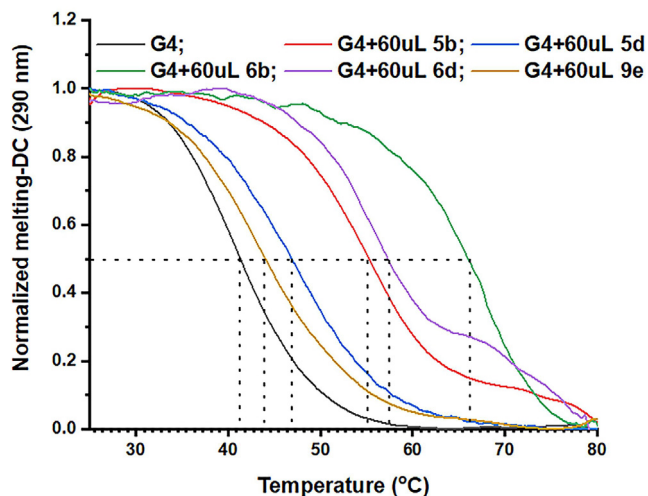
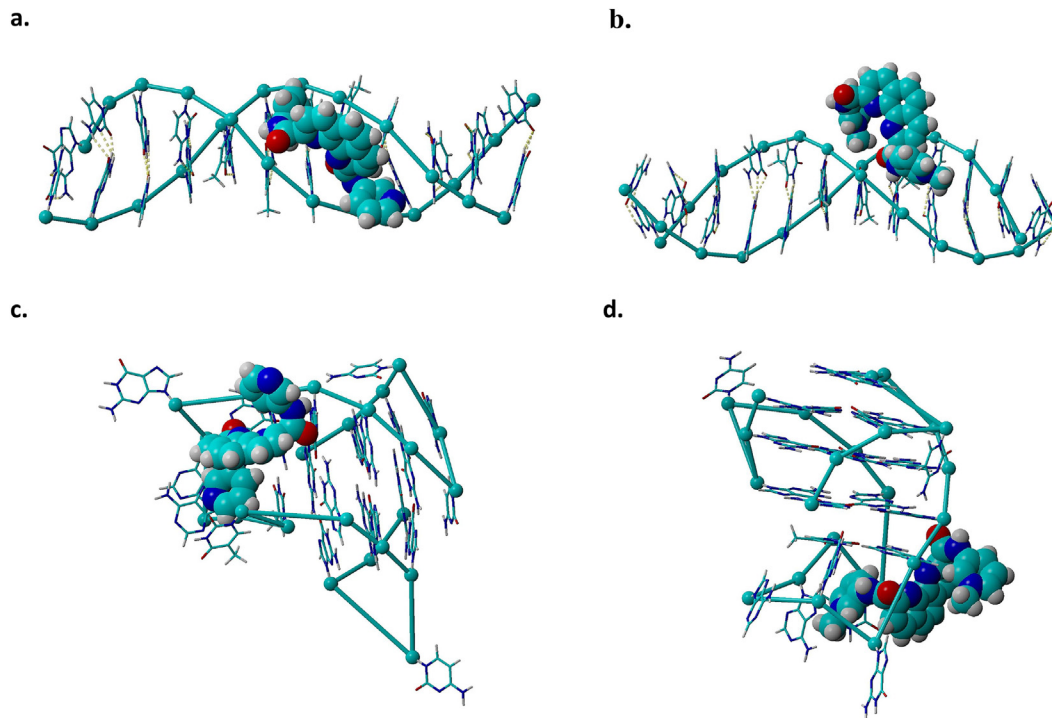


Fig. 3. CD melting profiles of the G4-DNA in the absence (black line) and in presence of compounds **5b**, **5d**, **6b**, **6d** and **9e**.

the two nitrogen atoms of the amide groups at the positions 2 and 9 of 1,10-phenanthroline, showed excellent antiproliferative activity. Even if by comparison with **5b**, the dimethylated derivative **6b** has a diminished potency in terms of anticancer activity, it demonstrated the best ability to bind and stabilize selectively the G-quadruplex DNA structure in the CD and CD melting experiments. Also mono-*N*-methylated compound **6d** displayed to be a good stabilizing ligand for G4-DNA suggesting that a positive charge is important for a better interaction with G-quadruplex structures. Also, the position of amino group on the appended heterocycles proved very important, all tested compounds showing anticancer activity having the amino group in position 3 or 8. Increasing the molecule flexibility due to the four methylene bridges present in the structure of derivatives **9** proved detrimental for the growth inhibitory properties on the cancer cells. Computational docking studies revealed preferential binding affinities of the investigated compounds toward dsDNA except for compound **6b** which demonstrated lower  $K_d$  value for G-quadruplex rather than for dsDNA. In case of **6b** the theoretically determined affinity to G-quadruplex is also supported by the melting point experimental data. In order to correlate the cytotoxic properties shown by compounds **6b** on

**Table 3** $\Delta T_m$  values obtained by using CD-melting experiments.

Ligand	Non-Methylated		Methylated		
	5b	5d	6b	6d	9e
$\Delta T_m$ (°C)	13	5	24	15	2

**Fig. 4.** MD sticks and balls rendering models of: 5b (ligand)/dsDNA (receptor-1) (a); 6b (ligand)/dsDNA (b); 5b/G-quadruplex 2F8U (receptor-2) (c); 6b/G-quadruplex 2F8U (d).**Table 4**

Values of binding energy and dissociation constants.

Ligand	dsDNA-Ligand		2F8U-Ligand	
	$E_b$ (kcal/mol)	$K_d$ (nM)	$E_b$ (kcal/mol)	$K_d$ (nM)
5b	-8.24	904.35	-8.24	905.87
5d	-10.57	17.898	-9.57	96.46
6b	-8.48	609.27	-8.72	405.65
6d	-10.57	18.86	-10.37	24.96
9e	-8.70	420.29	-8.63	471.40

some cancer cells and a possible inhibition of telomerase and to find the exact cellular effect, further studies have to be conducted.

### CRediT authorship contribution statement

**Anda-Mihaela Craciun:** Investigation, Writing - original draft, Writing - review & editing. **Alexandru Rotaru:** Investigation, Writing - original draft, Writing - review & editing. **Corneliu Cojocaru:** Investigation, Writing - original draft, Validation. **Ionel I. Mangalagiu:** Validation. **Ramona Danac:** Conceptualization, Supervision, Writing - original draft, Writing - review & editing.

### Declaration of competing interest

The authors declare no conflict of interest associated with this publication.

### Acknowledgements

The authors gratefully acknowledge National Cancer Institute (NCI) for biological evaluation of compounds on their 60-cell panel: the testing was performed by the Developmental Therapeutics Program, Division of Cancer Treatment and Diagnosis (the URL to the Program's website: <http://dtp.cancer.gov/>). We also thank the POSCCE-O 2.2.1, SMIS-CSNR 13984-901, Project no. 257/28.09.2010, CERNESIM, for the NMR experiments. This work was also supported by a grant of the Ministry of Research and Innovation, CNCS - UEFISCDI, project number PN-III-P4-ID-PCCF-2016-0050, within PNCDI III.

### Appendix A. Supplementary material

Supplementary data to this article can be found online at <https://doi.org/10.1016/j.saa.2020.119318>.

### References

- [1] S. Kumar, M.K. Ahmad, M. Waseem, A.K. Pandey, Drug targets for cancer treatment: An overview, *Med. Chem.* 5 (2015) 115–123, <https://doi.org/10.4172/2161-0444.1000252>.
- [2] S.A. Ohnmacht, S. Neidle, Small-molecule quadruplex-targeted drug discovery, *Bioorg. Med. Chem. Lett.* 24 (2014) 2602–2612, <https://doi.org/10.1016/j.bmcl.2014.04.029>.
- [3] Y. Qin, L.H. Hurley, Structures, folding patterns, and functions of intramolecular DNA G-quadruplexes found in eukaryotic promoter regions, *Biochimie* 90 (2008) 1149–1171, <https://doi.org/10.1016/j.biochi.2008.02.020>.

- [4] S. Balasubramanian, H.L. Hurlley, S. Neidle, Targeting G-quadruplexes in gene promoters: a novel anticancer strategy?, *Nat. Rev. Drug. Discov.* 10 (2011) 261–275, <https://doi.org/10.1038/nrd3428>.
- [5] G. Pennarum, C. Granotier, L.R. Gauthier, D. Gomez, F. Hoffschir, E. Mandine, J.F. Riou, J.L. Mergny, P. Mailliet, F.D. Boussin, Apoptosis related to telomere instability and cell cycle alterations in human glioma cells treated by new highly selective G-quadruplex ligands, *Oncogene* 24 (2005) 2917–2928, <https://doi.org/10.1038/sj.onc.1208468>.
- [6] D. Gomez, J.L. Mergny, J.F. Riou, Detection of telomerase inhibitors based on G-quadruplex ligands by a modified telomeric repeat amplification protocol assay, *Cancer Res.* 62 (2002) 3365–3368.
- [7] J. Amato, R. Morigi, B. Pagano, A. Pagano, S.A. Ohnmacht, A. De Magis, Y.P. Tiang, G. Capranico, A. Locatelli, A. Graziadio, A. Leoni, M. Rambaldi, E. Novellino, S. Neidle, A. Randazzo, Toward the development of specific G-quadruplex binders: Synthesis, biophysical, and biological studies of new hydrazine derivatives, *J. Med. Chem.* 59 (2016) 5706–5720, <https://doi.org/10.1021/acs.jmedchem.6b00129>.
- [8] N.W. Kim, Clinical implications of telomerase in cancer, *Eur. J. Cancer* 33 (1997) 781–786, [https://doi.org/10.1016/S0959-8049\(97\)00057-9](https://doi.org/10.1016/S0959-8049(97)00057-9).
- [9] P. Boukamp, N. Miranica, Telomeres rather than telomerase a key target for anti-cancer therapy?, *Exp. Dermatol.* 16 (2007) 71–79, <https://doi.org/10.1111/j.1600-0625.2006.00517.x>.
- [10] D. Sun, L.H. Hurlley, The importance of negative superhelicity in inducing the formation of G-quadruplex and i-motif structures in the c-Myc promoter: implications for drug targeting and control of gene expression, *J. Med. Chem.* 52 (2009) 2863–2874, <https://doi.org/10.1021/jm900055s>.
- [11] J.F. Riou, L. Guittat, P. Mailliet, A. Laoui, E. Renou, O. Petitgenet, F. Megnin-Chanet, C. Helene, J.L. Mergny, Cell senescence and telomere shortening induced by a new series of specific G-quadruplex DNA ligands, *Proc. Natl. Acad. Sci. U.S.A.* 99 (2002) 2672–2677, <https://doi.org/10.1073/pnas.052698099>.
- [12] J.Q. Hou, J.H. Tan, X.X. Wang, S.B. Chen, S.Y. Huang, J.W. Yan, S.H. Chen, T.M. Ou, H.B. Luo, D. Li, L.Q. Gu, Z.S. Huang, Impact of planarity of unfused aromatic molecules on G-quadruplex binding: Learning from isaindigotone derivatives, *Org. Biomol. Chem.* 9 (2011) 6422–6436, <https://doi.org/10.1039/C1OB05884C>.
- [13] S. Maiti, P. Saha, T. Das, I. Bessi, H. Schwalbe, J. Dash, Human telomeric G-quadruplex selective fluoro-isoquinolines induce apoptosis in cancer cells, *Bioconjugate Chem.* 29 (2018) 1141–1154, <https://doi.org/10.1021/acs.bioconjchem.7b00781>.
- [14] A. Rescifina, C. Zagni, M.G. Varrica, V. Pistara, Recent advances in small organic molecules as DNA intercalating agents: Synthesis, activity, and modeling, *Eur. J. Med. Chem.* 74 (2014) 95–115, <https://doi.org/10.1016/j.ejmech.2013.11.029>.
- [15] S. Neidle, D.E. Thurston, Chemical approaches to the discovery and development of cancer therapies, *Nat. Rev. Cancer* 5 (2005) 285–296, <https://doi.org/10.1038/nrc1587>.
- [16] R.B. Silverman, *The organic chemistry of drug design and drug action*, ed. Elsevier Academic Press, London, 2004.
- [17] T.P. Pradeep, R. Barthwal, A 4:1 stoichiometric binding and stabilization of mitoxantrone-parallel stranded G-quadruplex complex established by spectroscopy techniques, *J. Photochem. Photobiol. B* 162 (2016) 106–114, <https://doi.org/10.1016/j.jphotobiol.2016.06.019>.
- [18] D. Monchaud, P. Yang, L. Lacroix, M.P. Teulade-Fichou, J.L. Mergny, A metal-mediated conformational switch controls G-quadruplex binding affinity, *Angew. Chem. Int. Ed. Engl.* 47 (2008) 4858–4861, <https://doi.org/10.1002/anie.200800468>.
- [19] A. De Cian, E. DeLemos, J.L. Mergny, M.P. Teulade-Fichou, D. Monchaud, Highly efficient G-quadruplex recognition by bisquinolinium compounds, *J. Am. Chem. Soc.* 129 (2007) 1856–1857, <https://doi.org/10.1021/ja067352b>.
- [20] W.J. Chung, B. Heddi, F. Hamon, M.P. Teulade-Fichou, A.T. Phan, Solution structure of a G-quadruplex bound to the bisquinolinium compound Phen-DC (3), *Angew. Chem. Int. Ed.* 53 (2014) 999–1002, <https://doi.org/10.1002/anie.201308063>.
- [21] A. Wei, Y. Wang, M. Zhang, Synthesis and binding studies of novel di-substituted phenanthroline compounds with genomic promoter and human telomeric DNA G-quadruplexes, *Org. Biomol. Chem.* 11 (2013) 2355–2364, <https://doi.org/10.1039/C3OB27426H>.
- [22] A.F. Larsen, M.C. Nielsen, T. Ulven, Tetrasubstituted phenanthrolines as highly potent, water-soluble, and selective G-quadruplex ligands, *Chem. Eur. J.* 18 (2012) 10892–10902, <https://doi.org/10.1002/chem.201200081>.
- [23] M.C. Nielsen, A.F. Larsen, F.H. Abdikadir, T. Ulven, Phenanthroline-2,9-bistriazoles as selective G-quadruplex ligands, *Eur. J. Med. Chem.* 72 (2014) 119–126, <https://doi.org/10.1016/j.ejmech.2013.11.027>.
- [24] L. Wang, Y. Wen, J. Liu, J. Zhou, C. Li, C. Wei, Promoting the formation and stabilization of human telomeric G-quadruplex DNA, inhibition of telomerase and cytotoxicity by phenanthroline derivatives, *Org. Biomol. Chem.* 9 (2011) 2648–2653, <https://doi.org/10.1039/C0OB00961J>.
- [25] J.E. Reed, S. Neidle, R. Vilar, Stabilisation of human telomeric quadruplex DNA and inhibition of telomerase by a platinum-phenanthroline complex, *Chem. Commun.* 42 (2007) 4366–4368, <https://doi.org/10.1039/B709898G>.
- [26] N.M. Gueddouda, M.R. Hurtado, S. Moreau, L. Ronga, R.N. Das, S. Savrimoutou, S. Rubio, A. Marchand, O. Mendoza, M. Marchivie, L. Elmi, A. Chansavang, Y. Desplat, V. Gabelica, A. Bourdoncle, J.L. Mergny, J. Guillon, Design, Synthesis, and evaluation of 2,9-bis[(substituted-aminomethyl)phenyl]-1,10-phenanthroline derivatives as G-quadruplex ligands, *ChemMedChem* 12 (2017) 146–160, <https://doi.org/10.1002/cmdc.201600511>.
- [27] S. Wu, L. Wang, N. Zhang, Y. Liu, W. Zheng, A. Chang, F. Wang, S. Li, D. Shangguan, A bis(methylpiperazinylstyryl)phenanthroline as a fluorescent ligand for G-quadruplexes, *Chem. Eur. J.* 22 (2016) 6037–6047, <https://doi.org/10.1002/chem.201505170>.
- [28] L. Popovici, R.M. Amarandi, I.I. Mangalagiu, V. Mangalagiu, R. Danac, Synthesis, molecular modelling and anticancer evaluation of new pyrrolo[1,2-b]pyridazine and pyrrolo[2,1-a]phthalazine derivatives, *J. Enz. Inhib. Med. Chem.* 34 (2019) 230–243, <https://doi.org/10.1080/14756366.2018.1550085>.
- [29] R. Danac, C.M. Al Matarneh, S. Shova, T. Daniloia, M. Balan, I.I. Mangalagiu, New indolizines with phenanthroline skeleton: Synthesis, structure, antimycobacterial and anticancer evaluation, *Bioorg. Med. Chem.* 23 (2015) 2318–2327, <https://doi.org/10.1016/j.bmc.2015.03.077>.
- [30] A.M. Oлару, V. Vasilache, R. Danac, I.I. Mangalagiu, Antimycobacterial activity of nitrogen heterocycles derivatives: 7-(pyridine-4-yl)-indolizine derivatives. Part VII, *J. Enzyme Inhib. Med. Chem.* 32 (2017) 1291–1298, <https://doi.org/10.1080/14756366.2017.1375483>.
- [31] C.M. Al Matarneh, R.M. Amarandi, A.M. Craciun, I.I. Mangalagiu, G. Zbancioc, R. Danac, Design, synthesis, molecular modelling and anticancer activities of new fused phenanthrolines, *Molecules* 25 (2020) 527, <https://doi.org/10.3390/molecules25030527>.
- [32] A.M. Chiorcea-Paquim, A. Dora, R. Pontinha, R. Eritja, G. Lucarelli, S. Sparapani, S. Neidle, A.M. Oliveira-Brett, Atomic force microscopy and voltammetric investigation of quadruplex formation between a triazole-acridine conjugate and guanine-containing repeat DNA sequences, *Anal. Chem.* 87 (2015) 6141–6149, <https://doi.org/10.1021/acs.analchem.5b00743>.
- [33] J. Dash, Z.A.E. Waller, G.D. Pantos, S. Balasubramanian, Synthesis and binding studies of novel diethynyl-pyridine amides with genomic promoter DNA G-quadruplexes, *Chem. Eur. J.* 17 (2011) 4571–4581, <https://doi.org/10.1002/chem.2010013157>.
- [34] V. Dharmodharan, S. Harikrishna, C. Jagadeeswaran, K. Halder, P.I. Pradeepkumar, Selective G-quadruplex DNA stabilizing agents based on bisquinolinium and bispyridinium derivatives of 1,8-naphthyridine, *J. Org. Chem.* 77 (2012) 229–242, <https://doi.org/10.1021/jo201816g>.
- [35] A. Gomez, R. Paterski, T. Lemarteleur, K. Shin-ya, J.L. Mergny, J.F. Riou, Interaction of telomestatin with the telomeric single-strand overhang, *J. Biol. Chem.* 279 (2004) 41487–41494, <https://doi.org/10.1074/jbc.M406123200>.
- [36] J.M. Kumar, M.M. Idris, G. Srinivas, P.V. Kumar, V. Meghah, M. Kavitha, C.R. Reddy, P.S. Mainkar, B. Pal, S. Chandrasekar, N. Nagesh, Phenyl 1,2,3-triazole-thymidine ligands stabilize G-quadruplex DNA, inhibit DNA synthesis and potentially reduce tumor cell proliferation over 3'-azido deoxythymidine, *PLOS ONE* 8 (2013), <https://doi.org/10.1371/journal.pone.0070798> e70798.
- [37] A.D. Moorhouse, S. Haider, M. Gunaratnam, D. Munnur, S. Neidle, J.E. Moses, Targeting telomerase and telomeres: a click chemistry approach towards highly selective G-quadruplex ligands, *Mol. Biosyst.* 4 (2008) 629–642, <https://doi.org/10.1039/B801822G>.
- [38] J.E. Moses, D.J. Ritson, F. Zhang, C.M. Lombardo, S. Haider, N. Oldham, S. Neidle, A click chemistry approach to C3 symmetric, G-quadruplex stabilising ligands, *Org. Biomol. Chem.* 8 (2010) 2926–2930, <https://doi.org/10.1039/C005055E>.
- [39] A. Rais, I.R. Gould, R. Vilar, A.J.P. White, D.J. Williams, Structural and theoretical studies of new ruthenium-amidato complexes with phenanthroline ligands containing H-bonding groups, *Eur. J. Inorg. Chem.* 9 (2004) 1865–1872, <https://doi.org/10.1002/ejic.200300809>.
- [40] R.H. Shoemaker, The NCI60 human tumour cell line anticancer drug screen, *Nat. Rev. Cancer* 6 (2006) 813–823, <https://doi.org/10.1038/nrc1951> (and references therein).
- [41] X. Zhang, Y. Wei, T. Bing, X. Liu, N. Zhang, J. Wang, J. He, B. Jin, D. Shangguan, Development of squaraine based G-quadruplex ligands using click chemistry, *Sci. Rep.* 7 (2017) 4766, <https://doi.org/10.1038/s41598-017-04344-x>.
- [42] H. Zhang, L. Zou, R. Li, M. Zhao, L. Ling, Hairpin probe for sequence-specific recognition of double-stranded DNA on Simian Virus 40, *Chem. Res. Chin. Univ.* 34 (2018) 28–32, <https://doi.org/10.1007/s40242-017-7152-4>.
- [43] Y. Li, R. Li, L. Zou, M. Zhang, L. Ling, Fluorometric determination of Simian virus 40 based on strand displacement amplification and triplex DNA using a molecular beacon probe with a guanine-rich fragment of the stem region, *Microchim. Acta* 184 (2017) 557–562, <https://doi.org/10.1007/s00604-016-2041-y>.
- [44] O. Trott, A.J. Olson, AutoDock Vina: improving the speed and accuracy of docking with a new scoring function, efficient optimization, and multithreading, *J. Comput. Chem.* 31 (2010) 455–461, <https://doi.org/10.1002/jcc.21334>.
- [45] YASARA, Yet Another Scientific Artificial Reality Application: Molecular graphics, modeling and simulation program, official web-site: <http://www.yasara.org/>.
- [46] HyperChem(TM) Release 8.0, Hypercube, Inc., 1115 NW 4th Street, Gainesville, Florida 32601, USA, official web-site: <http://www.hyper.com/>.
- [47] J. Dai, D. Chen, R.A. Jones, L.H. Hurlley, D. Wang, NMR solution structure of the major G-quadruplex structure formed in the human BCL2 promoter region, *Nucl. Acids Res.* 34 (2006) 5133–5144, <https://doi.org/10.1093/nar/gkl610>.
- [48] A. Krieger, K. Joo, J. Lee, J. Lee, S. Raman, J. Thompson, M. Tyka, D. Baker, K. Karplus, Improving physical realism, stereochemistry, and side-chain accuracy in homology modeling: Four approaches that performed well in CASP8, *Proteins* 77 (2009) 114–122, <https://doi.org/10.1002/prot.22570>.

- [49] A. Krieger, G. Koraimann, G. Vriend, Increasing the precision of comparative models with YASARA NOVA - a self-parameterizing force field, *Proteins* 47 (2002) 393–402, <https://doi.org/10.1002/prot.10104>.
- [50] F.W. Lewis, L.M. Harwood, M.J. Hudson, M.G.B. Drew, J.F. Desreux, G. Vidick, N. Bouslimani, G. Modolo, A. Wilden, M. Sypula, T.H. Vu, J.P. Simonin, Highly efficient separation of actinides from lanthanides by a phenanthroline-derived bis-triazine ligand, *J. Am. Chem. Soc.* 133 (2011) 13093–130102, <https://doi.org/10.1021/ja203378m>.
- [51] J. Shao, Y. Qiao, H. Lin, H.K. Lin, Rational design of novel benzimidazole-based sensor molecules that display positive and negative fluorescence responses to anions, *J. Fluoresc.* 19 (2009) 183–188, <https://doi.org/10.1007/s10895-008-0400-8>.
- [52] R. Rusu, A. Szumna, N. Rosu, C. Dumea, R. Danac, New triazole appended tert-butyl calix[4]arene conjugates: synthesis, Hg<sup>2+</sup> binding studies, *Tetrahedron* 71 (2015) 2922–2926, <https://doi.org/10.1016/j.tet.2015.03.060>.
- [53] S. Haider, S. Neidle, *Methods in molecular biology*, in: P. Baumann (Ed.), *G-Quadruplex DNA*, Human Press, Springer, New York Dordrecht Heidelberg London, Methods and protocols, 2010.
- [54] S.B. Chen, Q.X. Shi, D. Peng, S.Y. Huang, T.M. Ou, D. Li, J.H. Tan, L.Q. Gu, Z.H. Huang, The role of positive charges on G-quadruplex binding small molecules: Learning from bisaryldiketene derivatives, *Biochim. Biophys. Acta* 2013 (1830) 5006–5501, <https://doi.org/10.1016/j.bbagen.2013.07.012>.
- [55] S.R. Liao, C.X. Zhou, W.B. Wu, T.M. Ou, J.H. Tan, D. Li, L.Q. Gu, Z.S. Huang, 12-N-Methylated 5,6-dihydrobenzo[c]acridine derivatives: A new class of highly selective ligands for c-myc G-quadruplex DNA, *Eur. J. Med. Chem.* 53 (2012) 52–63, <https://doi.org/10.1016/j.ejmech.2012.03.034>.
- [56] H.Y. Liu, A.C. Chen, Q.K. Yin, Z. Li, S.M. Huang, G. Du, J.H. He, L.P. Zan, S.K. Wang, Y.H. Xu, J.H. Tan, T.M. Ou, D. Li, L.Q. Gu, Z.S. Huang, New disubstituted quinoline derivatives inhibiting Burkitt's lymphoma cell proliferation by impeding c-MYC Transcription, *J. Med. Chem.* 60 (2017) 5438–5454, <https://doi.org/10.1021/acs.jmedchem.7b00099>.
- [57] K. Yadav, P.N. Rao Meka, S. Sadhu, S.D. Guggilapu, J. Kovvuri, A. Kamal, R. Srinivas, P. Devayani, B.N. Babu, N. Nagesh, Telomerase inhibition and human telomeric G-quadruplex DNA stabilization by a  $\beta$ -carboline-benzimidazole derivative at low concentrations, *Biochemistry* 56 (2017) 4392–4404, <https://doi.org/10.1021/acs.biochem.7b00008>.
- [58] S.K. Noureini, H. Esmaeili, F. Abachi, S. Khiali, B. Islam, M. Kuta, A.A. Saboury, M. Hoffmann, J. Sponer, G. Parkinson, S. Haider, Selectivity of major isoquinoline alkaloids from *Chelidonium majus* towards telomeric G-quadruplex: A study using a transition-FRET (t-FRET) assay, *Biochim. Biophys. Acta Gen. Subj.* 2017 (1861) 2020–2030, <https://doi.org/10.1016/j.bbagen.2017.05.002>.
- [59] C.B. Sun, T. Tang, H. Uludag, J.E. Cuervo, Molecular dynamics simulations of DNA/PEI complexes: Effect of PEI branching and protonation state, *Biophys. J.* 100 (2011) 2754–2763, <https://doi.org/10.1016/j.bpj.2011.04.045>.
- [60] J. Ziebarth, Y.M. Wang, Molecular dynamics simulations of DNA-polycation complex formation, *Biophys. J.* 97 (2009) 1971–1983, <https://doi.org/10.1016/j.bpj.2009.03.069>.